Fire Safety Journal 141 (2023) 103986

Contents lists available at ScienceDirect

Fire Safety Journal

journal homepage: www.elsevier.com/locate/firesaf

Fire spread in a large compartment with exposed cross-laminated timber and open ventilation conditions: #FRIC-02 - Exposed wall and ceiling

Andreas Sæter Bøe [a,d,*], Kathinka Leikanger Friquin [b], Daniel Brandon [c], Anne Steen-Hansen [a,d], Ivar S. Ertesvåg [e]

[a] Department of Civil and Environmental Engineering, Faculty of Engineering, NTNU – Norwegian University of Science and Technology, Trondheim, Norway
[b] Department of Architecture, Materials and Structures, SINTEF Community, Trondheim, Norway
[c] RISE Fire Research, Lund, Sweden
[d] RISE Fire Research AS, Trondheim, Norway
[e] Department of Energy and Process Engineering, Faculty of Engineering, NTNU – Norwegian University of Science and Technology, Trondheim, Norway

ARTICLE INFO

Keywords:
CLT
Fire spread
Large-scale
Compartment fire
Second flashover
Delamination
Facade fire
External flame

ABSTRACT

Cross-laminated timber (CLT) is becoming increasingly popular due to its many advantages. However, it has been shown that exposed CLT can have a significant effect on fire dynamics and spread rates. Further studies are therefore needed to better understand the impact of CLT to fire safety. Two large-scale CLT compartment fire experiments (95 m^2) representing a modern office building have been performed, #FRIC-01 and #FRIC-02. This paper presents the second experiment, #FRIC-02, with exposed CLT on the back wall and the ceiling. The fire developed fast and spread across the room in less than 3.5 min from ignition of the wood crib on the floor and in 1.5 min after the ignition of the ceiling. Large external flames were observed, despite the compartment being well-ventilated. The 5-layer CLT, which comprised a 40 mm thick exposed outer layer and was face-bonded using a common European polyurethane adhesive, exhibited glue-line integrity failure and led to a second flashover after a significant period of decay. Subsequent layers of 20 mm also delaminated before the fire was manually extinguished after 3 h. Compared to #FRIC-01, the fire spread rate was faster, and temperatures, charring rates, heat release rates and external flames were higher.

1. Introduction

In recent years, cross-laminated timber (CLT) has become the preferred choice of many architects, entrepreneurs and building owners due to its aesthetic look and ability to sequester carbon dioxide. Besides all the positive sides of CLT, it is well-known that exposed timber can impact fire dynamics and the growth rate of potential fires [1–3].

There is a strong architectural drive to leave the timber structure visible, which can sometimes, dependent on the regulations, be implemented without risk-mitigating measures such as limitations of exposed wood, sprinklers, surface coatings/impregnations, and limitations of compartment dimensions. Where such measures are not taken or cannot sufficiently be relied upon, sufficient insight into the impact on fire development can be important. The effect of an exposed CLT ceiling has been shown to increase the fire spread rate, which in large floor plan compartments can lead to fire growth rates [4,5] that are typically not accounted for in European design standards [6].

In the Code Red experiments [4,5], the fire spread across a 352 m^2 compartment and developed into a full flashover in 5 and 8 min. This was significantly faster than in similar experiments without a CLT ceiling [7,8]. In #FRIC-01 [9], however, ignition of the CLT ceiling took longer. Parameters that likely led to this difference are the lower flame height of the wood crib fire relative to the ceiling height, the larger opening factor and the higher window head, allowing less smoke to accumulate under the ceiling. After the ignition of the ceiling at 32.5 min, the fire spread back and forth across the room through four flashing waves, in which the wood crib fire grew larger after each wave. The fully developed fire was reached 13 min after the ignition of the ceiling. This can still be considered fast, as several similar fire experiments without exposed CLT have used hours to travel the same distance [10,11]. Despite the floor area of Code Red being almost four times larger than #FRIC-01 (352 m^2 vs. 95 m^2), there were several similarities in the experimental setups, like the oblong geometry (34.3 m × 10.3 m × 3.0 m vs. 18.8 m × 5.0 m × 2.5 m), the large continuous wood crib and the

* Corresponding author.
E-mail addresses: andreas.s.boe@ntnu.no, andreas.boe@risefr.no (A.S. Bøe).

https://doi.org/10.1016/j.firesaf.2023.103986
Received 31 March 2023; Received in revised form 17 August 2023; Accepted 17 September 2023
Available online 27 September 2023

exposed CLT ceiling. As the fire development in #FRIC-01 significantly differed from that in the Code Red experiments, it increased insight into the strong dependence on the fire scenario, compartment design and the complexity of the fire dynamics. There is, however, a complete lack of data on large-scale fire experiments of large floor plan compartments with a combination of exposed wall and ceiling surfaces. Several compartment fire experiments (7 m^2 [12], 17.5 m^2 [13], 42 m^2 [14] and 48 m^2 [15]) have compared how different combinations of exposed surfaces affect the fire dynamics. However, all of these are of dimensions that are not representative of large floor plan compartments, and none of these experiments has studied how the fire spread rate changes with different combinations of exposed surfaces. Thus, there is a knowledge gap on how an exposed wall, in addition to a ceiling, would affect the fire spread rate in a large compartment.

Another possible consequence of having exposed CLT is the prolonged fire duration, which might occur due to delamination (also known as glue-line integrity failure or premature char fall-off) or gypsum board fall-off. In both cases, fresh preheated wood becomes exposed to the fire, and the phenomenon is often recognised by a rapid increase in the temperature and heat release rate. This effect has been observed in several experiments [14,16].

Avoiding delamination has been considered beneficial for achieving self-extinction of compartment fires, and lately, there has been an increased focus on developing adhesives that do not exhibit delamination [4,15,17].

With a regular polyurethane adhesive, several parameters affect whether delamination occurs, like the outer layer thickness of the CLT, the duration of the fire, the burning time of the CLT, and whether the CLT continue smouldering after the extinguishment of flames. It should be noted that there are examples of fires with delamination that have not caused a second flashover [9,14,18]. There are also experiments where self-extinction has been achieved without using a heat-resistant adhesive [9,12,16,18,19].

Delamination and self-extinction of CLT have been extensively studied at bench scale [19–21], and there are also a few experiments from small to large-scale [12–15,18] which have studied these related phenomenon. It has been found that the number of exposed CLT surfaces and their orientation to each other impact whether self-extinction or delamination occur due to feedback mechanisms between the exposed CLT. However, due to the few really large-scale experiments, there are still knowledge gaps on how feedback mechanisms affect self-extinction and delamination in large compartments with different orientations of exposed CLT.

As many modern wooden buildings have one or several surfaces with exposed wood, it is essential to better understand the feedback mechanisms between exposed CLT surfaces and the variable fuel load and how this interaction changes the fire spread and fire dynamics in the compartment. Hence, two large-scale experiments have been conducted in a well-ventilated, large, open-spaced compartment with exposed CLT. The experiments aimed to study how fire dynamics and fire spread rates change with two different configurations of exposed CLT. In #FRIC-01 [9], the ceiling was exposed, while in #FRIC-02, a long wall and the ceiling were exposed. The results of #FRIC-02 are presented and discussed in this paper.

2. Methods

2.1. Methodology

The effects of exposed cross-laminated timber surfaces on fire development and spread in large, open-plan compartments with open ventilation conditions are studied through a large-scale experiment. The methodology of #FRIC-02 is identical to that of #FRIC-01. Several methods have been used to describe the fire and measure the effects of the timber; analysis of video recordings, measurements of the temperatures in the compartment, heat flux towards surfaces, and calculations of the heat release rates for the variable fuel and CLT.

2.2. Experimental setup

The experimental setup was almost identical to #FRIC-01. Hence, the information given here summarises the method and provides key information and relevant changes compared to #FRIC. For more details on the experimental setup and analysis methods, readers are referred to the article describing #FRIC-01 [9].

2.2.1. Compartment

The compartment's inner dimension was 18.8 m × 5.0 m × 2.52 m (L × W × H), and CLT elements were used in all walls and the ceiling. In contrast to #FRIC-01, this experiment (#FRIC-02) had both the ceiling (89.3 m^2) and the back wall (47.1 m^2) exposed. Images of the compartment are shown in Fig. 1.

The CLT of the back wall and ceiling had a thickness of 140 mm and consisted of 5 layers. The outer layers were 40 mm thick with a board width of 140 mm, whereas the three intermediate layers were 20 mm thick and had a board width of 90 mm. The CLT panels were made of Norwegian spruce and glued with Loctite Purbond HB S, a regular polyurethane (PUR) adhesive. The density of the CLT elements was approx. 484 kg/m^3 (based on measurement of one element with 13% moisture content).

The compartment had four large window openings on the front wall, with a total opening area of 17.0 m × 2.2 m = 37.4 m^2. This corresponds to an opening factor of 0.18 $m^{1/2}$. Windows 1–4 are enumerated from the left. Thermally inert facade walls with dimensions 2.45 m high and 5.0 m wide were positioned above Windows 2 and 4.

In case of heavy rain showers during the construction period, standing water would accumulate next to the back wall outside the compartment. To avoid significant water absorption into the CLT back wall under such circumstances, a 130 mm × 50 mm wooden plank was laid directly on the ground as a sacrificial layer, and the wall elements were positioned on top of that. A fire sealant was added to the wall-wall connections, the wall-ceiling connections, and between the ground and the bottom plank. By mistake, there was no sealant between the wall elements and the bottom plank. This likely led to tiny gaps of ~1–2 mm at some locations along the bottom of the wall.

#FRIC-02 was conducted one week after #FRIC-01. The walls were undamaged after being used in #FRIC-01 and therefore reused, while a new CLT ceiling was provided. The wall had been partly dried during the fire in #FRIC-01 but regained its moisture content after having been left with the wet gypsum boards for two days after the experiment. The moisture content of the exposed wall was measured to 14.1% ± 0.5% (standard deviation, n = 36) the day before the experiment took place. In comparison, the moisture content of the new CLT ceiling was 13.1% ± 1.1% (standard deviation, n = 36). The moisture content (dry value) was measured by a calibrated moisture meter.

The end walls were covered by two layers of 15 mm fire-rated gypsum boards type F [22]. The glulam beam was reused as it was undamaged from #FRIC-01, but the ceramic fibre insulation protecting it was replaced. The concrete floor was covered with new insulation boards of stone wool.

2.2.2. Wood cribs

The variable fuel was represented by two wood cribs, one long continuous wood crib (15.5 m × 2.8 m × 0.2 m) and a smaller wood crib (1.0 m × 2.8 m × 0.2 m) positioned on a scale (Fig. 1). The load cells of the scale were protected from heat by stone wool insulation (2 × 30 mm) on top and aerated concrete blocks on the sides.

The two cribs were built similarly to #FRIC-01 with 50 mm × 50 mm wood sticks in four alternating layers. The wood used was Norwegian spruce, with an average density of 486 kg/m^3 ± 40 kg/m^3 (standard deviation, n = 25) and a total mass of 2075 kg for both cribs. The average moisture content was 14.5%, with 12.8% ± 1.2% (standard

Fig. 1. Experimental setup from the outside and inside of the compartment. The small wood crib on the scale is on the right side of the left image.

deviation, n = 20) and 16.2% ± 1.3% (standard deviation, n = 20) for the short and long sticks, respectively. The fuel load density was 353 MJ/m^2 per floor area.

2.2.3. Ignition

Also in this experiment, the fire was ignited by heptane. 14 metal trays (150 × 220 × 50 mm) were positioned on the floor next to the wood crib on the left end. The trays were filled with 0.7 L of heptane in each and positioned 70 mm from each other. The two first bottom sticks of the crib were removed and put on top of the crib, so there were four stick layers at the beginning of the crib as well. 150 mm of the trays were positioned under the wood crib. This setup deviates slightly from the setup in #FRIC-01, and the reason for the change will be elaborated in Section 4.5.

2.2.4. Weather conditions

The wind conditions were measured by a local weather station positioned 15 m northeast of the compartment. The wind direction was diagonally from behind the right-end corner, with a wind velocity of 2 m/s and a gust velocity of 5–8 m/s, see Table 1. The gust velocity represents short-lived (<20 s) increases in the wind velocity. The wind and gust angles are given as where the wind is originating, with North as 0°. The orientation of the compartment is shown in Fig. 2.

2.3. Instrumentation and measurements

Most of the instrumentation, including thermocouples (TCs), plate thermometers (PTs), bidirectional probes, and gas sensors, were reused from #FRIC-01. Damaged TCs were replaced by new ones. The instrumentation setup is shown in Fig. 3-Fig. 5 and consists of 120 thermocouples (TCs) of type K 1.5 mm diameter, 24 standard plate thermometers (PTs), four bidirectional probes, and three gas sensors. The PTs were facing inwards into the compartment. The positions of the TCs, PTs etc., are described by the X, Y, and Z-directions, where X is the longitudinal direction starting from the left side of the compartment, Y is the transverse horizontal direction, and Z is the vertical direction. The zero-point for X, Y, and Z is located on the floor inside the left end wall in the window opening.

Table 1
Wind condition from the ignition of wood crib.

Time [min]	Wind angle [°]	Wind velocity [m/s]	Gust angle [°]	Gust velocity [m/s]
0	55	2	104	5
5	29	2	125	5
10	3	3	323	8
15	42	2	14	4
20	62	2	79	5
25	4	2	308	8
30	69	2	83	6

TCs were also embedded into the CLT wall and ceiling at 0, 10, 20, 30 and 40 mm depths parallel to the isotherm. They were installed at three locations, X = 4.7, 9.5 and 14.3 m (Fig. 4). The TCs embedded in the back wall were installed at 1.1 m height, and the TCs embedded in the ceiling were installed along the centreline of the ceiling, Y = 2.5 m. The embedded TCs were used to determine the char depth of the CLT and charring rate throughout the experiment. For this, the 300 °C isotherm was considered the location of the charring front [23]. After the experiment, the final char depth was measured on some of the CLT elements in the wall and the ceiling.

The incident heat flux was determined using a method described by Wickström [24]. The gas velocities were measured by bidirectional probes, as explained by Ref. [14], originating from Ref. [25]. Oxygen (O_2), carbon monoxide (CO) and carbon dioxide (CO_2) concentrations were measured by a gas analyser at three different locations, shown in Figs. 3–5.

The method to estimate the heat release rate (HRR) from the wood crib was inspired by Rackauskaite et al. [7] and consisted of three steps: 1) determine the mass loss rate (MLR) per unit length of the wood crib, 2) integrate over wood crib length, 3) convert MLR to HRR.

In contrast to the method of Rackauskaite et al. [7], the MLR per unit length (here: 50 mm) in this experiment was based on a real mass loss rate measurement from the 1.0 m × 2.8 m wood crib positioned on a scale at the right end of the compartment, i.e., opposite of the ignition side (Fig. 1). The HRR was approximated through $\dot{Q} = \dot{m}\,\Delta H_C \chi$, where the MLR ($\dot{m}$) is multiplied by the net heat of combustion (lower heating value) (ΔH_C) and a combustion efficiency factor (χ). A combustion efficiency of 0.8 and a net heat of combustion of 16.0 MJ/kg were used.

The MLR for the ceiling and wall were determined based on the calculated charring rates of the CLT. The mass loss rate was then estimated based on the average charring rate for each 10 mm into the wood, the density and the surface area of the CLT. The net heat of combustion values for the wood crib and CLT were derived from the net calorific value of 18.66 MJ/kg for dry wood [26] and a moisture content (dry value) [27] of 14.5% for the wood crib, 13.1% for the ceiling, and 14.1% for the wall. The resulting net heat of combustion was 16.0 MJ/kg for the wall and the wood crib and 16.2 MJ/kg for the ceiling.

The HRR of the external flame out of Window 4 was estimated utilising a linear relation between flame volume and HRR of 1.505 ± 0.183 MW/m^3 [28]. The volume of the flame was estimated by measuring the outline of the external flame from the side and the average flame width

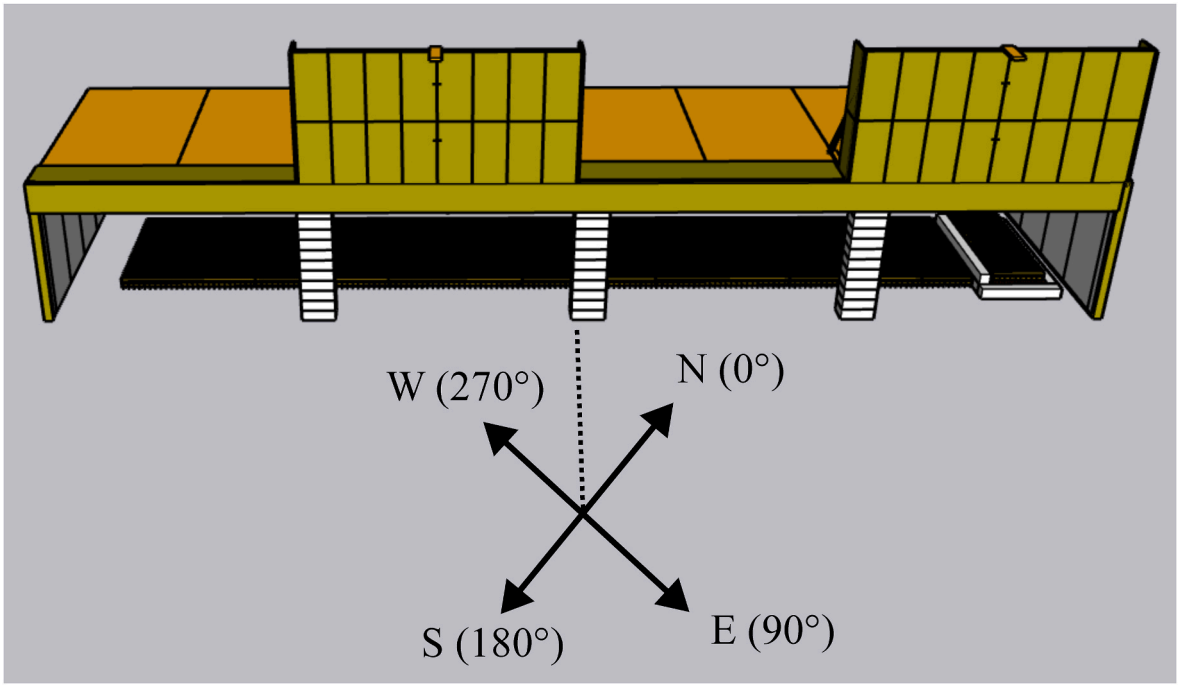

Fig. 2. Orientation of the compartment.

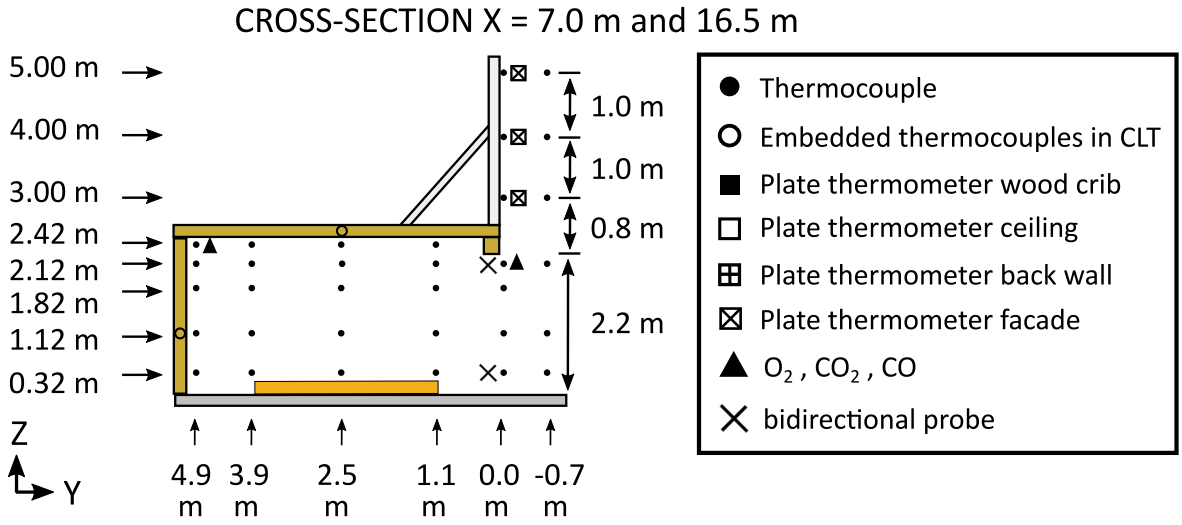

Fig. 3. Instrumentation in the YZ-plane (cross-section) at X = 7.0 m and 16.5 m. For X = 16.5 m, only gas measurements in the window opening. Figure from #FRIC-01.

from the front through a photo editing program. The dimensions were found by comparing them to a known reference in the images.

3. Results

3.1. Fire development

The wood crib was ignited from the left end, as described in Section 2.2.3. For the first one and a half minutes, the flames tilted towards the leftmost end wall with a flame height of 1–2 m. Ignition of the ceiling occurred at 01:42 (mm:ss) (Fig. 6). At the time of CLT ceiling ignition, 0.15 m of the length of the crib was burning together with the heptane. At 02:10, a smoke layer was covering the entire ceiling, and the flames underneath the ceiling had grown to cover approx. 4 m of the ceiling length. At 02:20, the wood crib fire was about the same size as before the ceiling ignited, while the ceiling fire now covered approx. One-third (~6 m) of the ceiling area. The unignited wood crib was, at this point, strongly preheated by the burning ceiling, which is seen by the cloud of evaporated moisture in Fig. 6.

The first observation of the wall burning was at 02:00. At 02.30, a few meters of the upper third of the wall was burning at the left side of the compartment. From this point on, the fire spread rapidly, see Fig. 7. At 03:05, the fire had spread to about half the wood crib and three-fourths of the ceiling. At 03:10, large external flames emerged out of Window 4, and the entire length of the wood crib ignited at 03:13. This time is here defined as flashover as it was the first occurrence of all materials simultaneously burning. After the flashover, external flames appeared from all window openings, with the largest flames out of Window 4, farthest away from the ignition point.

After the flashover, the fire burned intensely with large external

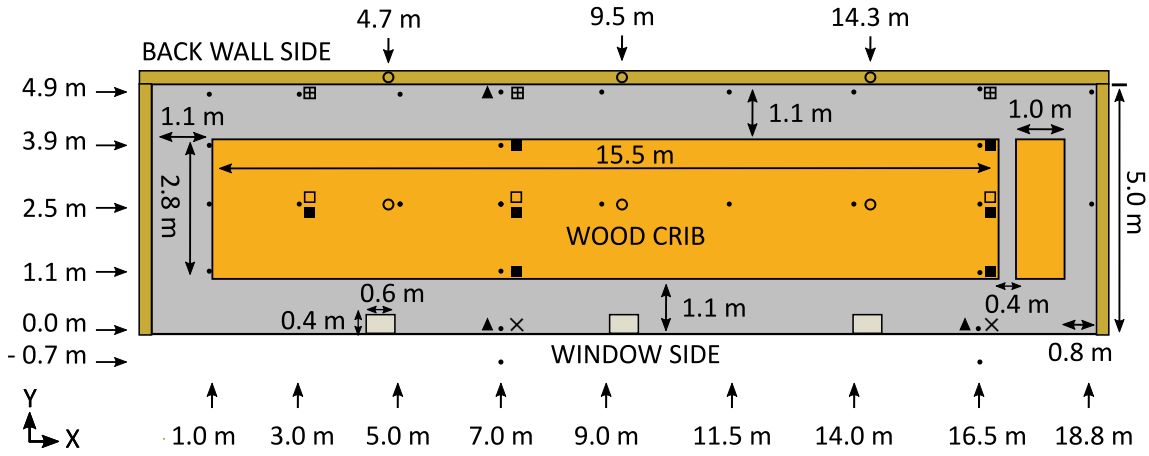

Fig. 4. Instrumentation in the XY-plane (plan view). For symbols, see Fig. 3. Figure from #FRIC-01.

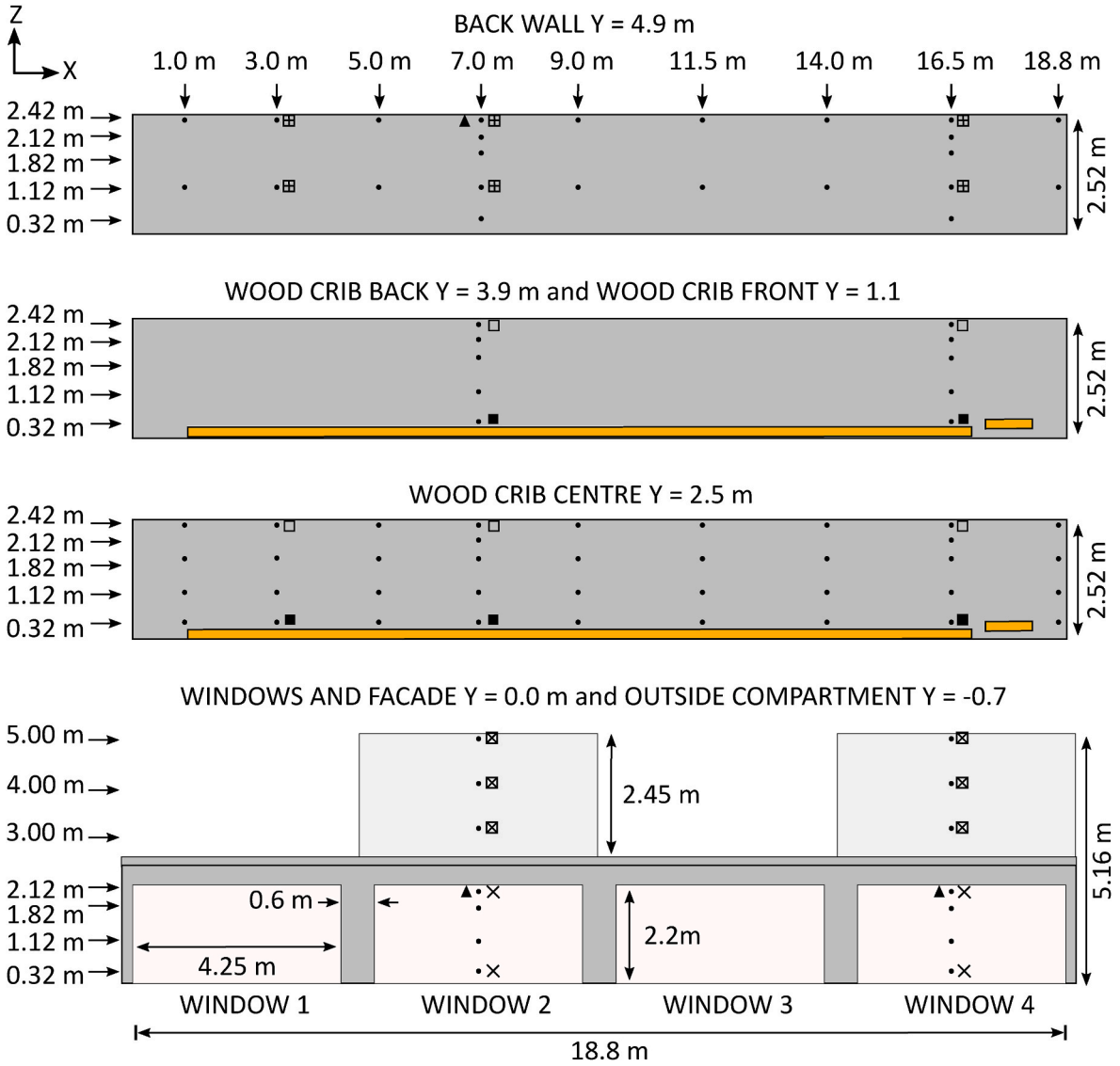

Fig. 5. Instrumentation in XZ-plane. For Y = −0.7 m, only TCs are used, not gas sensors or bidirectional probes. For symbols, see Fig. 3. Figure from #FRIC-01.

flames for about 8 min. The flames at the CLT wall and ceiling gradually extinguished from the left end of the compartment (ignition side) from about 13 min, see Fig. 8. At 16 min, all flames in the wall and ceiling were extinguished, while the wood crib was still burning. From 24 min, the crib burnt with discontinuous flames, and the last flames disappeared after 50 min.

Fig. 6. Flame spread below the ceiling after ignition of CLT seen from the left side of the compartment. Time (mm:ss).

At 66 min, small flames were observed at two different positions on the CLT of the back wall. At this point, there was barely anything left of the wood crib. Over the next 4 min, several flames appeared both in the ceiling and the wall, see Figs. 9 and 10(a). At 74 min, the multiple small flames had grown to cover the entire height of the wall for approximately two-thirds of the length and half of the ceiling width, see Fig. 11. At 76 min, almost the entire compartment was burning, and external flames appeared from the window openings. In this period, many small (10–50 cm) and some larger (50–100 cm) pieces of delaminated boards fell down and caused a large heap of glowing embers on the floor, see Fig. 10(b). The intensity of the fire varied over the next 100 min and had an increasing trend right before it was manually extinguished after 175 min. A summary of the fire development is given in Table 2.

3.2. Compartment temperatures

Compartment temperatures based on PT measurements are shown in Fig. 12-Fig. 14. Compartment temperature maps based on the TC measurements in the XZ-plane are given in Fig. 15, and in the YZ-plane in Fig. 16-Fig. 17 for Windows 2 and 4. All PT temperatures had increased to 700–1000 °C after 4 min. The peak temperatures were reached at 7 min, with temperatures between 1010 and 1172 °C for all PT locations. The hottest areas were close to the end walls. The lowest temperatures were measured in the centre of the compartment at the middle height, X = 9 m, Z = 1.0–1.5 m, as seen in Fig. 15. From 3 to 8 min, there was a reversed temperature gradient at the back of the room, with a lower temperature at 2.4 m height than at 1.1 m height, as seen in Fig. 13. Large temperature differences were also seen in the cross-section through Window 2, see Fig. 16, where a defined temperature gradient was present from the lower height of the window to the back of the room. Through Window 4 (Fig. 17), this gradient was less pronounced, and the temperatures were almost uniform in the cross-section. During the most intense burning phase, i.e., 4–8 min, the temperature difference from the back wall to Window 2 at 1.1 m height was approximately 700–800 °C. The difference for the cross-section through Window 4 was only 200–300 °C.

At 12–18 min, the temperature dropped from 1135 to 810 °C for the maximum PT measurements and from 924 to 575 °C for the minimum PT measurements. The decay rate of the compartment temperatures in this period was 52 ± 10 °C/min on average. The extinguishment of flames at the CLT wall and ceiling started from the left end and was extinguished completely between 14 and 16 min, see Fig. 8. Visible flames extinguished at temperatures (PTs) between 805 and 845 °C and an incident heat flux of 70–84 kW/m^2.

From 18 min, a temperature increase was measured by all PTs in the ceiling and some of the PTs on the back wall and the wood crib, see Figs. 12–14. This increase lasted for about 5–8 min, and the peak values were reached at 22 min. This increase is also seen in Figs. 15–17. Except for this short-lived increase, the temperatures in the whole compartment decayed after the extinguishment of flames at the CLT. The temperatures next to the ceiling and the wall decreased almost linearly, with an average rate of 5.7 ± 0.1 °C/min over the next 50 min. The ceiling temperatures in the decay phase were uniform, with just minor differences along the Y-axis. In contrast, significant differences were seen for the wood crib temperatures, with lower temperatures at the window side.

Before the initiation of the second flashover, the temperatures in the compartment had cooled down for about an hour. The temperatures measured by PTs below the ceiling and on the back wall were 386–490 °C. The temperatures at the first glue line, i.e., 40 mm depth, at 70 min in the ceiling and the wall were 173–221 °C.

We define the onset of the second flashover as occurring at 76 min, although the right part of the wall was not included until after 78 min. In the transition to the second flashover, the wall and ceiling temperatures increased rapidly and peaked at approximately 1050 °C, almost as high as during the first flashover. The temperature distribution was less uniform, with a more apparent difference between the PTs of the wall, ceiling, and wood crib. After the second flashover, the temperature

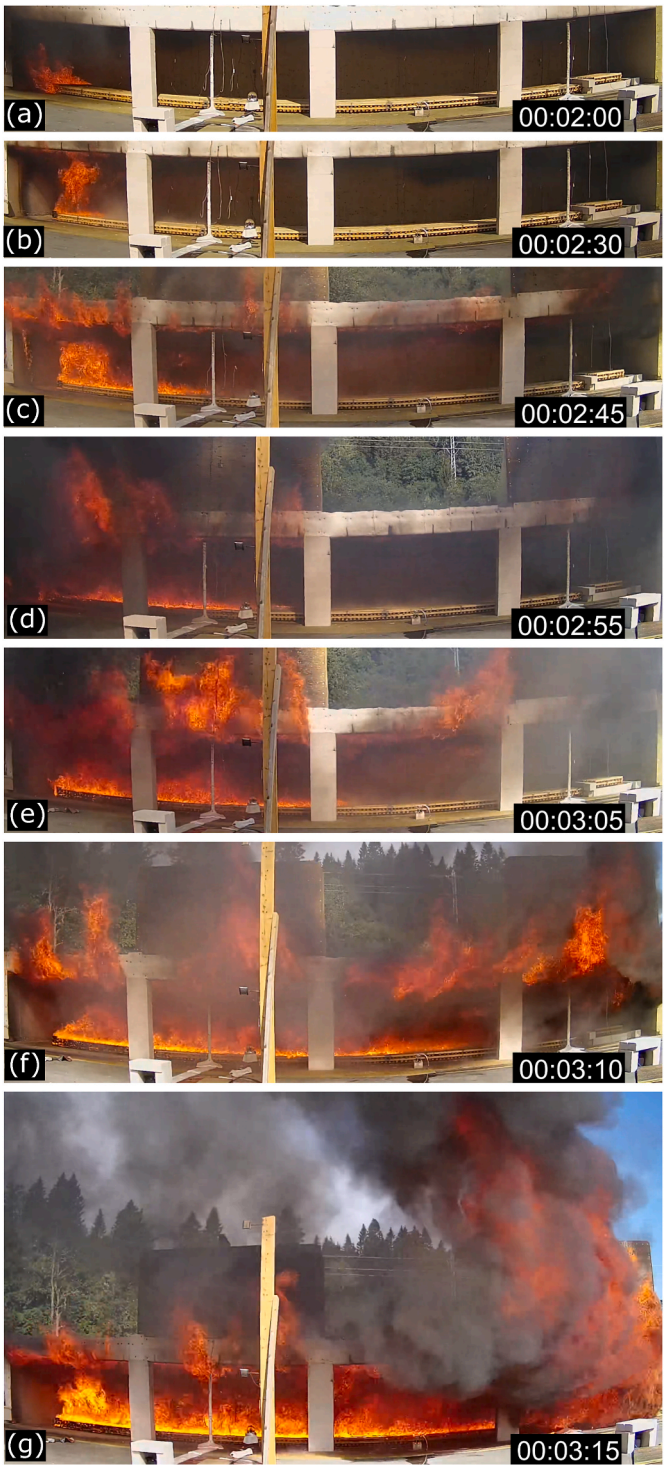

Fig. 7. (a)–(g) Fire spread across the compartment. Time (hh:mm:ss).

varied considerably but remained above 550 °C below the ceiling and 500 °C by the wall. The fire reached its minimum phase at approx. 128 min with all PT temperatures below 585 °C, corresponding to an incident heat flux of 19–28 kW/m^2. At this point, small flames covered a large part of the wall, see Fig. 9 (k). Visually, the fire intensity was at its minimum at 120 min, where only a few minor flames were present, see Fig. 9 (j). After this period, the temperatures and the fire intensity increased slowly until the fire was put out at 175 min. At this point, the temperatures were at their highest since 106 min.

3.3. External flames and facade temperatures

External flames were emerging from all window openings after flashover, but the size of the flames was non-uniform, with by far the largest flames appearing from Window 4, see Fig. 7 (g). The development of the external flames emerging from Window 4 is shown in Fig. 18. The flames were largest between 3 and 7 min and then gradually decreased to no flame. This is also shown in Fig. 19, where the height, volume and an estimated HRR are given.

Although short-lived, the maximum external flames from Window 4 were 6–8 m high from the ground, extending several meters above the facade wall, see Fig. 18. At maximum (Fig. 20), the flames were impinging on the facade to the top of the facade walls and then tilted away from the compartment with a ~45° angle. The depth of the external flame was approximately 3 m at the ceiling height but extended at maximum nearly 6 m from the facade at a higher point. The largest external flames had a volume of 45 ± 10 m^3, see Fig. 19 (b). Utilising the linear relation between external flame volume and HRR [28], the maximum HRR of the external flame was estimated to be 66 ± 20 MW.

Another characteristic of the flame from Window 4 was that it filled almost the entire window height for a part of the window in the most intense burning phase. Hence, the neutral plane was here almost at floor level. This can be observed several times in Fig. 18 and shown over time in Fig. 19.

The temperatures measured at the facade are shown in Fig. 21. The highest temperatures were measured above Window 4 between 3 and 9 min with peak PT temperatures around 1020 °C, 865 °C and 720 °C at 0.8, 1.8 and 2.8 m above the window soffit. The exposure to the facade was also significant during the second flashover but lower than during the first flashover.

The incident heat fluxes were calculated based on the PT and TC measurements, as described in Section 2.3 and given in Fig. 22. The heat flux above Window 4 was at its maximum between 3 and 9 min, with heat flux levels fluctuating between 125 and 175 kW/m^2. The maximum 30-s moving average was 156, 96 and 67 kW/m^2 for heights 0.8, 1.8 and 2.8 m above the window soffit of Window 4, respectively. At +0.8 m height, the maximum 30-s averaged value occurred at 6 min, while the maximum value for +1.8 and + 2.8 m occurred at 3.5 and 4 min, respectively. This confirms that the largest flames lasting 30 s were present shortly after flashover, although short-lived large flames were present also later. In comparison, the values above Window 2 were significantly lower, with a 30-s average of 64, 34 and 12 kW/m^2.

The velocities inwards at Z = 0.3 m and outwards at Z = 2.1 m through Windows 2 and 4 were found through measurements with bidirectional probes, as described in Section 2.3. Velocities for the most intense external flaming are given in Fig. 23. The synchronisation of the time might deviate slightly from the other graphs, as the TC for synchronisation was defective, and there was a short delay between the time at which the gas was sampled until it was measured by the sensor.

The 30 s maximum average velocities outwards from the compartment at Z = 2.1 m were approximately 8 m/s through Window 2 and 14 m/s through Window 4. The duration of the outward flow was shorter for Window 2 compared to Window 4. In the figure, the average inward velocities at Z = 0.3 m were approximately the same for Windows 2 and 4, with a velocity between 2 and 4 m/s, but with stronger fluctuations in Window 4. However, the bidirectional probe at 0.3 m height in Window 4 was not set up to measure reversed flows, i.e., outward flows, as this was not expected. Hence, the average inward flow in Window 4 is likely closer to zero than presented in the figure. Several of the bidirectional probes gave unreliable data after 8 min and were therefore not included in the analysis. The unreliableness is believed to have been caused by a hole in the connections due to heat exposure.

3.4. Fire spread across CLT and wood crib

The fire spread across the wood crib and ceiling was found through

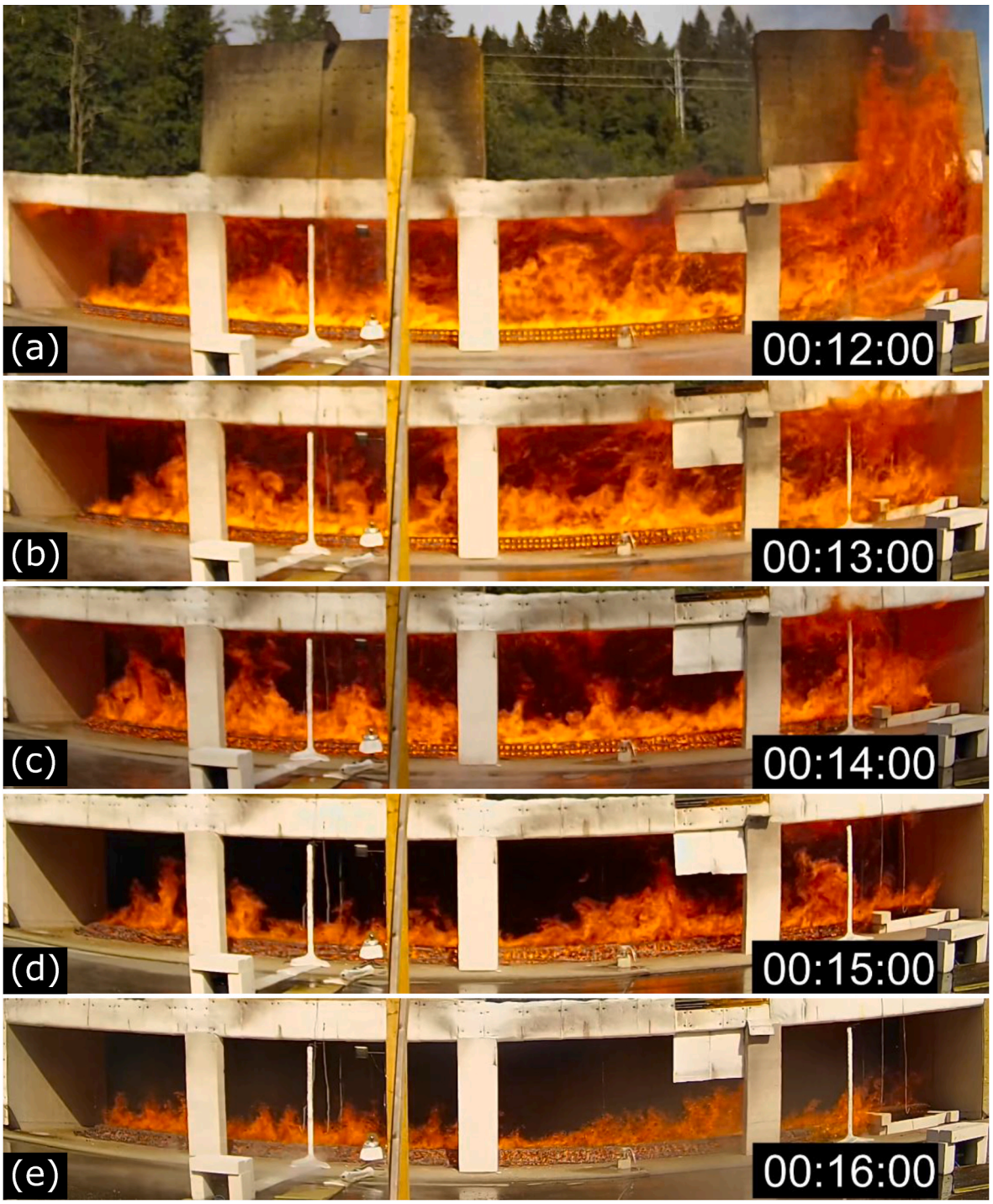

Fig. 8. (a)-(e) Development of self-extinguishment of CLT while wood crib was still burning. Time (hh:mm:ss).

video analysis, and an exponential curve matched well with the spread across the wood crib, Fig. 24. The fire spread rate was then found through the derivation of the exponential curve. The (harmonic) average fire spread rate across the wood crib from ignition was approx. 5.5 m/min (90 mm/s) and 11.7 m/min (195 mm/s) from the ignition of the ceiling. The average spread rate across the ceiling was approx. 15 m/min (250 mm/s). As shown in Fig. 24, the spread rate was increasing almost exponentially. This is visualised by comparing the fire development in Fig. 7 (e)–(g), where it took 3 min for the wood crib fire to cover half of the wood crib and just 10 s to travel across the second half of the crib.

Fire spread based on the TC temperatures is shown in Fig. 25, where a threshold of 600 °C is used to indicate flames. The flames spread first across the ceiling and the upper part of the wall, followed by ignition of the wood crib and the lower part of the wall at about the same time. At X = 7.0, the flames spread clearly from the top of the wall and downwards. This is also shown visually in Fig. 25. However, at X = 16.5, the entire height of the wall ignited within a few seconds. Compared to the visual observations of the fire spread, the 600 °C indicator gives a few seconds delay. Based on the temperature indicator, the average flame spread rate from X = 3.0–18.8 m ranged from 13 to 23 m/min.

Fig. 9. (a)–(l) Development of the second flashover. (j) Fire intensity at its minimum. (k) Fire intensity at minimum compartment temperature. Time (hh:mm:ss).

3.5. Gas measurements

Oxygen (O_2), carbon dioxide (CO_2), and carbon monoxide (CO) concentrations were measured at three different locations, as described in Section 2.3, and the results are given in Fig. 27. The O_2 concentration measured in Window 2 was not recorded due to a fault. The O_2 concentration shown is, therefore, calculated backwards from the CO and CO_2 concentrations. For short periods, both the CO and CO_2 reached the limits of the sensor, and the actual O_2 concentration will therefore be lower than what is shown in the figure. Measurements for Windows 2 and 4 are missing from 60 to 80 min and after 150 min.

The O_2 concentration measured at the window openings decreased rapidly after flashover and stabilised at 10% and 5% between 5 and 9 min for Windows 2 and 4, respectively. For a short period from 11 to 13 min, the O_2 concentration was 0% through Window 4. From 15 min, the O_2 concentration increased steadily until the second flashover occurred. During the second flashover, the O_2 was, in the most intense burning phase, reduced to 0% but was between 7 and 16% most of the time. In the back of the room, O_2 was at its lowest of 18.4% just after flashover. This level is higher than expected, possibly caused by a small leakage in the tube collecting the gas. Measurements from this location should therefore be considered with caution. The CO concentration was higher than 5000 ppm in all three locations from 4 to 16 min. From this point, the CO concentration was reduced quickly and is related to the extinguishment of flames at the CLT wall and ceiling. From 25 min, the CO concentration increased steadily in Window 2. The CO-sensor in Window 4 stopped working after 15 min.

3.6. Charring of CLT

Charring rates for the CLT are given in Table 3 and Table 4 and were measured as described in Section 2.3. For the first 40 mm, the charring followed a clear trend with a high charring rate for the first 10 mm, followed by a decreasing rate for each extra 10 mm into the wood.

The final char depths were measured at different locations and are shown in Figs. 28 and 29. The arithmetic average of the final char depth across the CLT back wall was 97 mm with a standard deviation of 13 mm and 104 mm with a 7 mm standard deviation for the CLT ceiling. Charring in the ceiling was noticeably non-uniform, with less charring at the right end of the compartment in both the wall and the ceiling. The char depth was also deeper at the bottom compared to the top of the wall. In the ceiling, the charring was evidently more pronounced close to the wall compared to the window side. The difference was more than 30 mm in several places. An example is given in Fig. 30, where the charring in some areas of the ceiling close to the window side has only reached the 3rd layer ($<$80 mm), while close to the wall, the charring has in most places reached the 5th layer ($>$100 mm). In the figure, two areas are entirely burnt through close to the window side. The main reason for this was insufficient extinguishing in the inner corner between the glulam beam and the ceiling at the end of the experiment. This area was hard to reach by water when standing on the outside. Extinguishing was not performed from the inside of the compartment due to safety concerns. Due to this insufficient extinguishing, smouldering was still occurring for several hours, and the CLT reignited in at least two locations on top of the compartment above the glulam beam. The reignition was discovered 7–8 h after the end of the experiment, but it is unknown exactly when the reignition happened. A heavy rain shower and additional manual extinguishing stopped further combustion after 8 h. The ongoing smouldering next to the glulam beam is the reason for the outliers at Y = 0.3 m in Fig. 29. Complete charring (140 mm) was also seen at the bottom of the wall several places from 60 min, see Fig. 31.

3.7. Delamination and second flashover

Both in #FRIC-01 and here, delamination was defined to occur when a part of the outer layer detaches from the second layer due to the

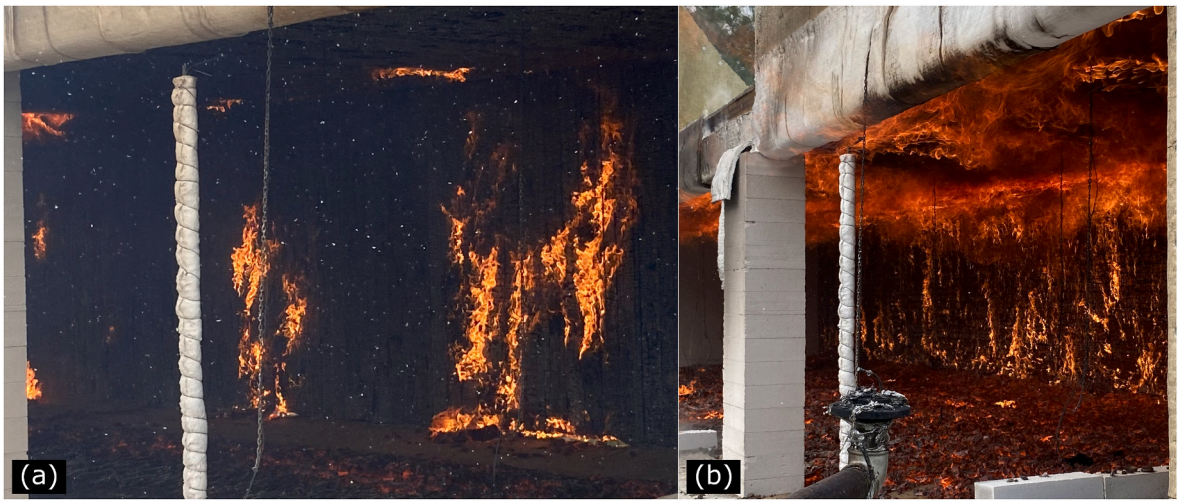

Fig. 10. (a) The first flames leading to the second flashover appeared at the lower part of the back wall and in the innermost part of the ceiling. (b) Ceiling and wall burning, and glowing embers on the floor from falling pieces. Photos were taken at 70 min (a) and 93 min (b).

Fig. 11. In the transition to the second flashover, the full height of the back wall was burning before half of the ceiling width had been included in the fire. Photo from 74 min.

Table 2
Summary of fire development.

Time (min)	Observation	Figure
0	Heptane trays were ignited.	
1.75–3.25	The fire spread first across the ceiling and the top of the wall and finally across the wood crib and lower part of the wall.	Fig. 7
3.25–11	After the flashover, external flaming was highly inhomogeneous as most external combustion occurred out of Window 4.	Fig. 7
11–13	A clear reduction in external flaming, and the burning of the CLT wall on the left end was less intense.	Fig. 8
13–16	Extinction of the CLT wall and ceiling, starting from the left end, while the wood crib was still burning continuously.	
24–40	The wood crib burnt discontinuously.	
40–50	Tiny flames were present at a few locations but eventually died out.	
66–76	Development of flames on the back wall and the ceiling, leading to a second flashover.	Figs. 9–11
76–175	A continuous fire with varying degrees of intensity.	
175	Manual extinguishment of the fire.	

adhesive losing its integrity. Uncharred, preheated wood in the second layer was then exposed.

The small flames that appeared from 66 to 70 min (Fig. 10) rapidly grew in size, and at 74 min, most of the wall and half of the ceiling were burning, see Fig. 11. A distinct change in the burning behaviour occurred between 74 and 76 min, see Fig. 9. At 74 min, the flames were mainly originating from the burning of the fresh wood of the second layer. However, at 76 min, the intensity of the flames had increased significantly, and from the images, it is evident that also the first layer was burning again. The incident heat flux towards the wall increased in this period from approx. 40 kW/m^2 to 104 kW/m^2. At this point, external flames emerged from all window openings. At 78 min, the right end of the compartment was also included in the fire.

The most intense fire lasted just a few minutes (76–81 min). After this, the fire intensity varied a lot, as seen in Fig. 9. An intermediate minimum was reached around 90 min before the fire reached a new peak at 104–106 min. At 120 min, the fire reached its minimum with only minor flames present. However, again the fire grew in intensity and at 175 min, just before it was manually extinguished, it was at its most intense since 106 min (see Figs. 9 and 12) and showed no signs of being close to self-extinction.

The varying fire intensity and temperatures were related to the delamination of the second, third and fourth lamella, which all were 20 mm thick. The estimated times for the char front to reach the different layers and cause delamination is given in Table 5. The values were calculated from the average charring rate of 0.52 mm/min for the ceiling (Table 3) and 0.67 mm/min for the wall (Table 4). Fig. 31 shows the gas temperature next to the back wall, and distinct temperature peaks are present at almost identical intervals after the second flashover. The occurrence of these peaks matches well with the estimated times for the char front progress in Table 5.

3.8. Mass loss rate and heat release rate

3.8.1. Mass loss rate

The mass loss rate of the wood crib was determined as described in Section 2.3. An exponentially decaying function was fitted to the measured mass loss of the crib on the scale and then derived to get the MLR, see Fig. 33. Compared to the real MLR averaged over 30 s, the estimated MLR based on the fitted curve gave a good match.

The MLR per unit (50 mm) length was then found by dividing the MLR from the small crib by 20. The MLR per unit length was combined with the fire spread across the wood crib, see Fig. 24, to obtain the total MLR and HRR for the wood crib. This process is explained in more detail

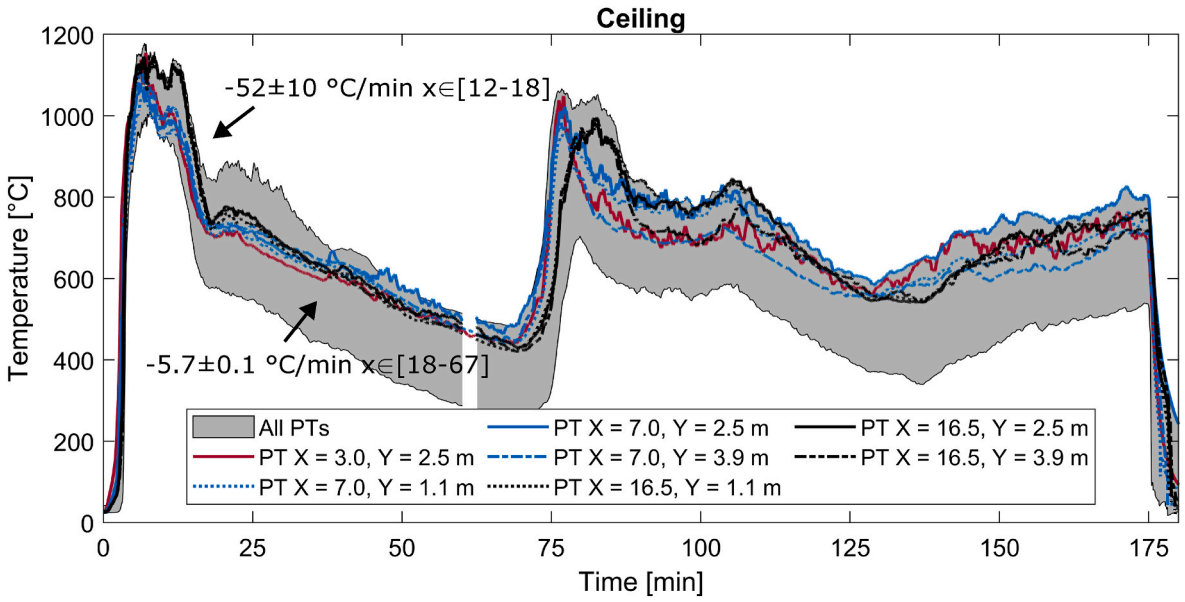

Fig. 12. Temperatures 100 mm below the ceiling measured by PTs facing downwards. The grey area covers all measurements by PTs in the compartment. X and Y represent the position of the PTs.

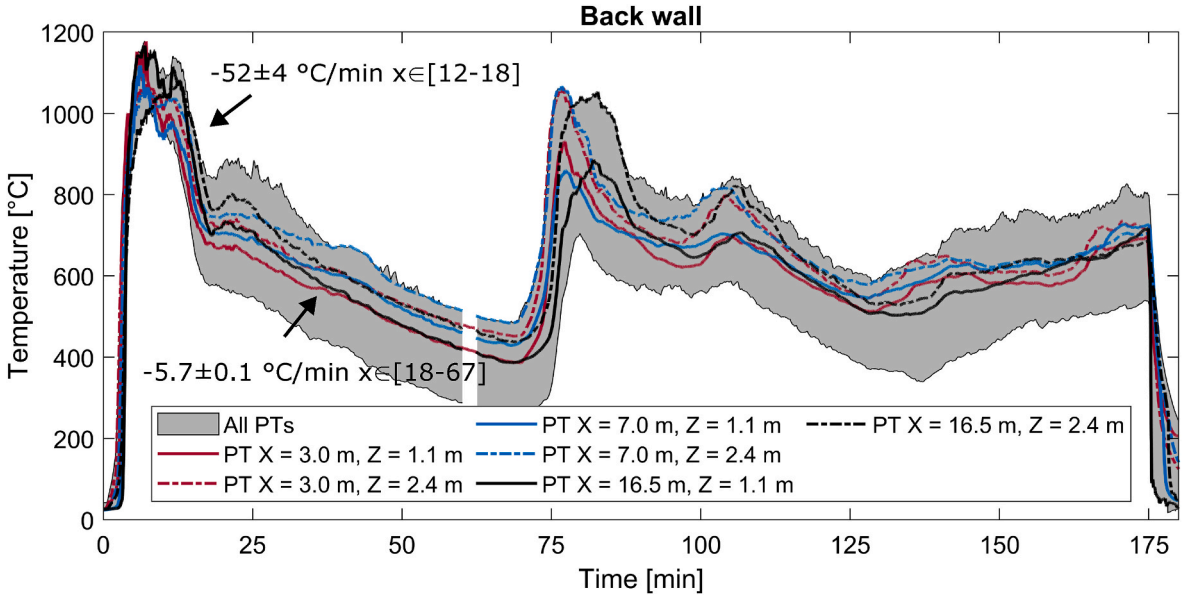

Fig. 13. Temperatures 100 mm in front of the back wall measured by PTs facing away from the wall. The grey area covers all measurements by PTs in the compartment. X and Z represent the position of the PTs.

in #FRIC-01 [9]. The estimated maximum MLR of the wood crib based on this method was 2.69 kg/s, corresponding to a burning rate of 7.28 g/(s m^2), where m^2 is the surface area of the wood sticks. The theoretical maximum mass loss and burning rate were estimated to be 2.81 kg/s and 7.60 g/(s m^2), which assumes that the entire crib starts to burn simultaneously and at a similar rate as the crib on the scale.

The mass loss rate of the CLT was based on the charring rates of the CLT, see Tables 3 and 4. The estimated maximum mass loss rate was 1.03 kg/s and 1.90 kg/s for the wall and ceiling, respectively. This corresponds to a burning rate of 0.022 kg/m^2s and 0.021 kg/m^2s.

3.8.2. *Heat release rate*

The HRR for the wood crib, the CLT and these combined are shown in Fig. 34, where the maximum HRR was estimated to be 73 MW. The HRR of the CLT was obtained from the charring rate of 10 mm intervals, and the curve, therefore, has a stepwise development. The average HRR after the second flashover was 3.5 MW for the back wall and 5.5 MW for the ceiling. The development of the HRR curve was considerably faster than the ultrafast t^2 curve [6], with a fire growth rate constant, t_α, of 27 s vs. 75 s. During the most intense burning phase (i.e., max HRR), the contribution from the wood crib was 35 MW (48%), 13 MW (18%) from the CLT wall, and 24.5 MW (34%) from the CLT ceiling.

With a combustion efficiency of 0.8, the area below the HRR curves should ideally equal 80% of the energy content of the initial wood crib mass (2075 kg), the burned mass of the CLT wall (2409 kg) and CLT ceiling (4188 kg). The area below the HRR for the wood crib was equal to 81% of the energy content of the initial wood crib mass, while the areas below the HRR curve for the CLT ceiling and wall were equal to 78% and 73% of the energy content of the mass of the burned CLT, respectively.

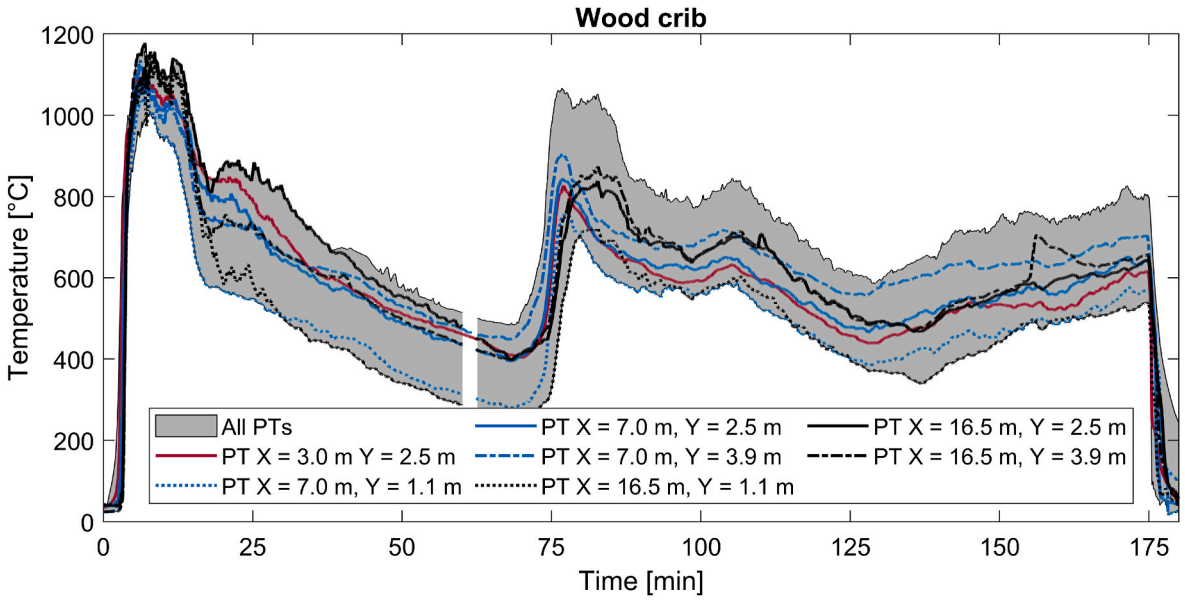

Fig. 14. Temperatures on top of the wood crib measured by PTs facing upwards. The grey area covers all measurements by PTs in the compartment. X and Y represent the position of the PTs.

4. Discussion

To our knowledge, this is the first large open-plan fire experiment combining an exposed CLT ceiling and wall. The contribution from the wall is clearly shown by comparing against the results of #FRIC-01 [9], which had a similar experimental setup, but with only the ceiling exposed.

The most important results from this experiment are the fast fire spread, the large and strongly non-uniform external flames, the second flashover after the long decay phase, and the non-uniform char depth. These results are discussed in more detail in the following sub-sections.

4.1. Fire spread

The fire developed very fast, and the wood crib fire spread across the room in 3 min and 13 s from ignition (5.5 m/min) and in 91 s from ignition of the ceiling (11.7 m/min). The fire under the ceiling reached the end of the compartment a few seconds earlier, with an average rate of 15 m/min from the ignition of the ceiling. The development of the fire spread rate was exponential, as seen in Fig. 24, indicating that the average spread rate could have been even faster in a longer compartment. The development of the total HRR was faster than the ultrafast t^2-curve and is considerably faster than the medium and fast fire growth rates suggested for different occupancies in Eurocode 1 [6]. This fire spread rate across the room was significantly faster than reported for most compartments with non-combustible surfaces, with a maximum rate of 1–2 m/min [7,8,29–31], as described in #FRIC-01 [9]. Compared to compartments with exposed CLT, the fire spread rate is even faster than the fastest spread rate in the Code Red experiments, in which the fire spread rate was 9.6 m/min across the wood crib and 12 m/min across the CLT ceiling from ignition of the ceiling [4]. A direct comparison to the spread rates of #FRIC-01 was not made here due to the pulsating behaviour of the fire spread across the ceiling and the crib. Still, there is no doubt that a CLT orientation with a ceiling and a wall facilitates a faster spread rate compared to just having the ceiling exposed.

Before the flashover, there was a clear movement of smoke and fire toward the far end of the compartment. This behaviour was due to the 0.36 m deep insulated glulam beam, which effectively guided the smoke towards the far end of the compartment. Thus, the position of beams under a ceiling will effectively contribute to what direction smoke, and later a fire, will spread. In addition, the height of the beam will affect the thickness of the smoke layer, and thereby the temperatures in, and radiation, from the smoke layer.

Fig. 6 gives a unique insight into the mechanisms of the fast fire spread. Shortly after ignition of the ceiling, a thick smoke layer formed below the ceiling. This smoke layer contained a large fraction of combustible gases (recognised by the black colour) and is a key factor for the flame spread below the ceiling, as discussed in #FRIC-01 [9]. The radiation from the burning ceiling preheated the CLT wall and the wood crib, which is seen by the cloud of evaporated moisture at 02:20 in Fig. 6. Shortly after, the wood crib fire started to spread rapidly.

At 02:20, it is noticeable how far the flames had spread under the ceiling, while the size of the wood crib was about unchanged since the ignition of the ceiling. This highlights that the contribution from the CLT (wall and ceiling) was the dominating factor for the fast fire spread, and not what type of moveable fuel that was present. In an actual building, the fire growth rate could be limited by the oxygen supply, which is ultimately controlled by whether the window glasses break or not. A large compartment volume, either by a large floor area or a high ceiling height, would compensate for the lack of window breakage for a certain time.

4.2. Charring rate and char depth

The charring rate was highest for the first 10 mm and was reduced for each subsequent 10 mm into the wood. The stepwise charring pattern was also seen in #FRIC-01 and can likely be explained by the initial rapid mass loss rate for combustion of wood, followed by a reduced rate when a char layer is formed [19,32]. The charring rates were also likely affected by the large variations in temperature and heat fluxes during the charring of the first 40 mm. The high charring rate for the first 10 mm did not influence the total charring rate much, but it had an impact on the fire spread rate and external flames as it contributed to a large amount of pyrolysis gases being produced the first minutes after ignition. Pyrolysis gases burnt inside the compartment contribute to higher temperatures and is a driving force for the fast fire spread. Unburned gases exiting the compartment burn as an external flame, which may spread the fire to the facade, a compartment above, or an opposite building.

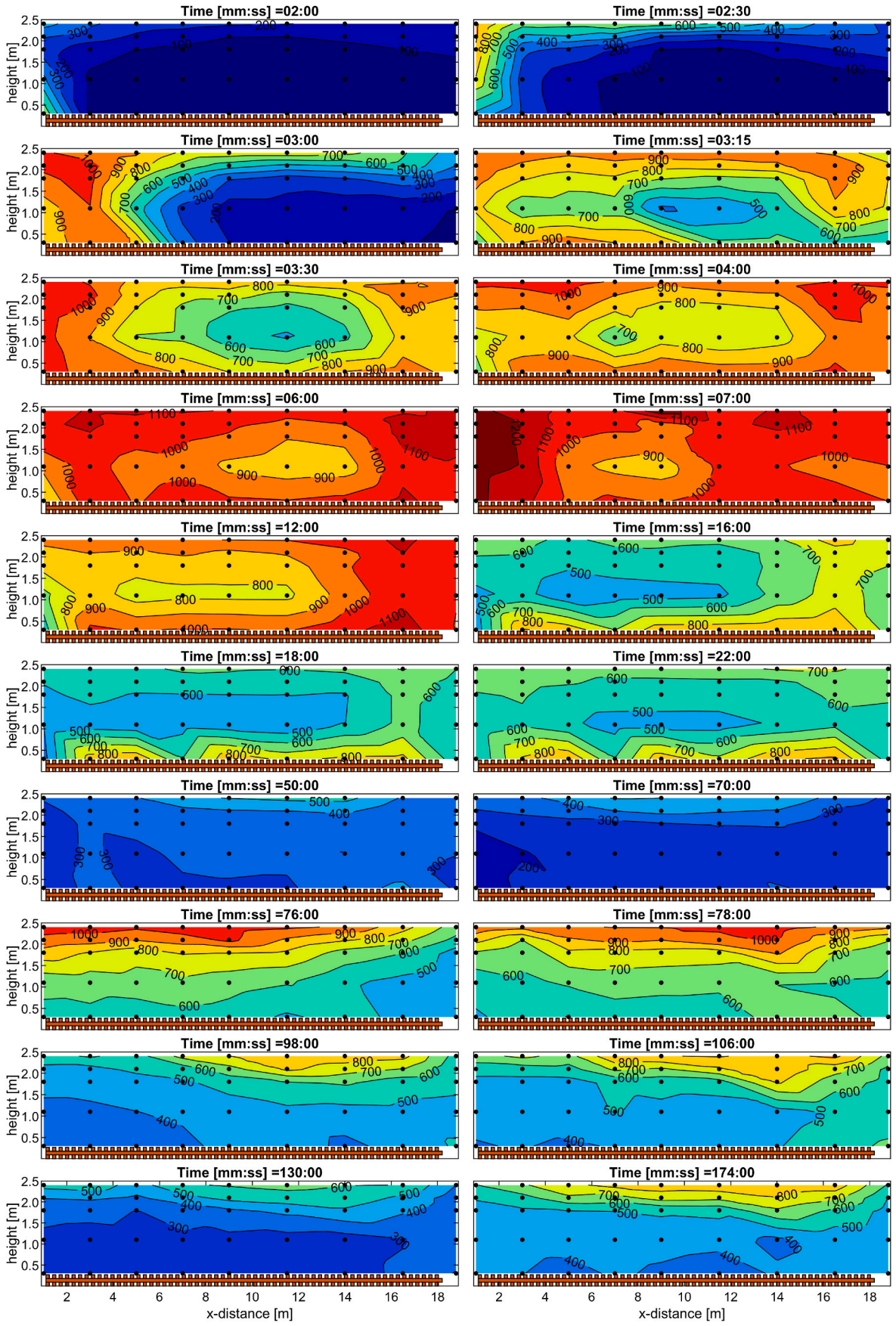

Fig. 15. Temperature map of XZ cross-section through the centre of the compartment (Y = 2.5 m).

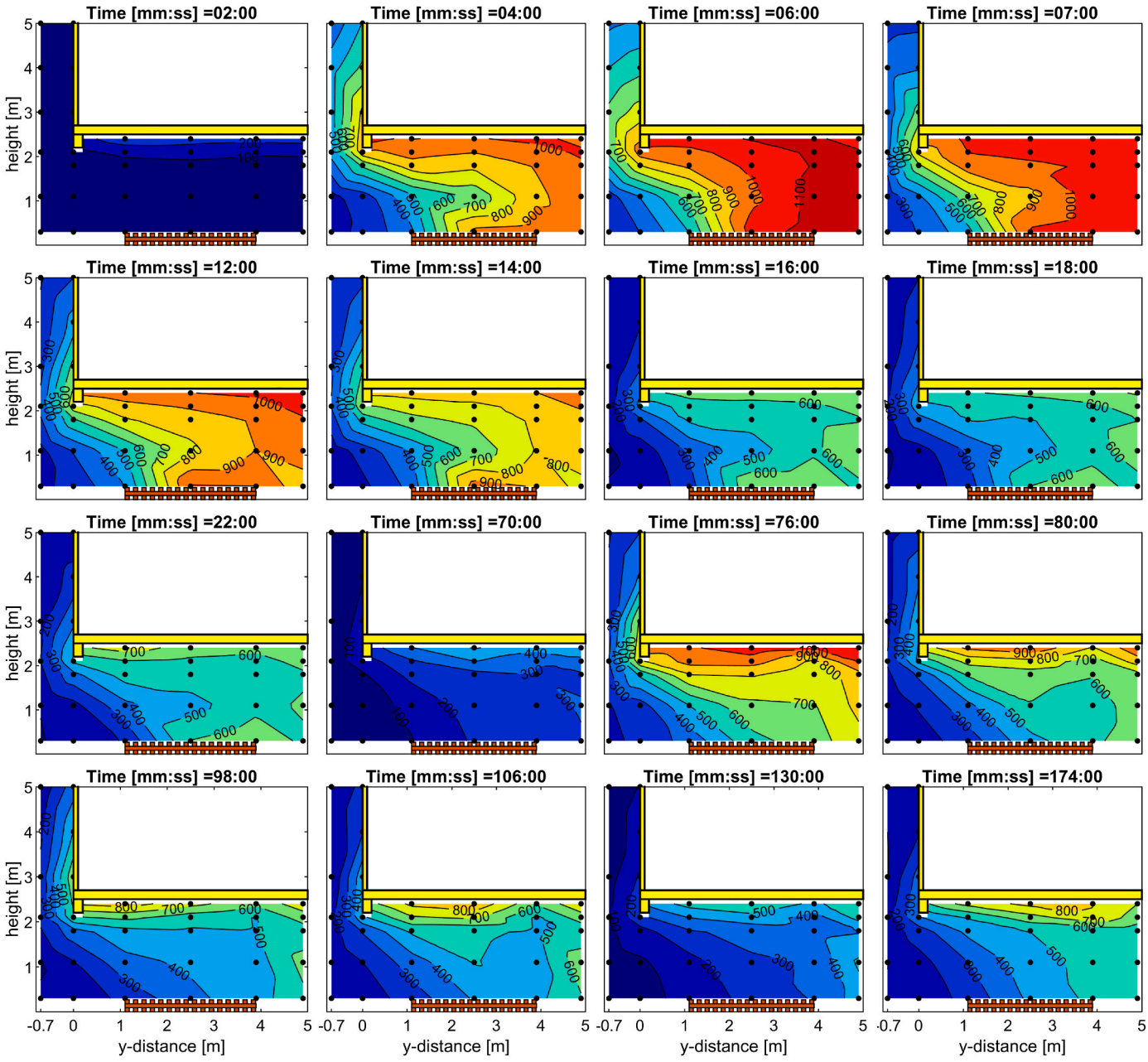

Fig. 16. Temperature map of YZ cross-section through the centre of Window 2 (X = 7.0 m).

The final char depth measured after the experiment was strongly non-uniform, with more charring on the bottom of the wall than the top and more pronounced for the part of the ceiling closest to the back wall. This is similar to #FRIC-01 but more distinct here. In addition, the charring of the wall was deeper than in the ceiling, 104 mm vs 97 mm. This corresponds with previous experiments, summarised by Mitchell et al. [3], where there is a clear trend of faster charring rates of the wall compared to the ceiling.

Furthermore, the development of the flames in the transition to the second flashover matches well with the char depth pattern shown in Figs. 28–30. This is apparent in Figs. 10(a) and Fig. 11, where the first flames leading to the second flashover appeared at the lower height of the wall and the innermost part of the ceiling. It was also clear that the wall had been more charred than the ceiling at this point, as most of the wall was burning, while just part of the ceiling had visible flames on the surface. In addition, the right end of the back wall and ceiling ignited last, as seen in Fig. 9 (e). Consequently, it appears that the non-uniform charring pattern, in general, had developed already before the onset of the second flashover.

The uneven charring is mainly believed to be due to the different oxygen concentrations [33] throughout the compartment. It is believed that the supply of oxygen entered the compartment at a low height through the window and was transported to the back of the wall, upwards along the wall and exiting out of the compartment below the ceiling. Along such a path, the oxygen concentration would be more and more diluted, with the lowest concentration when exiting the compartment below the window soffit. Given that this path of the oxygen is correct, it can explain the large differences in char depth between the wall and ceiling and of the ceiling and wall separately. In addition, the reduced charring at the right end of the compartment can also be explained by the low oxygen concentrations in the most intense burning phase of the fire. Increased charring could also have been caused by a higher heat flux or temperature [33]. The reversed temperature gradient close to the wall in the most intense burning phase of the fire could have

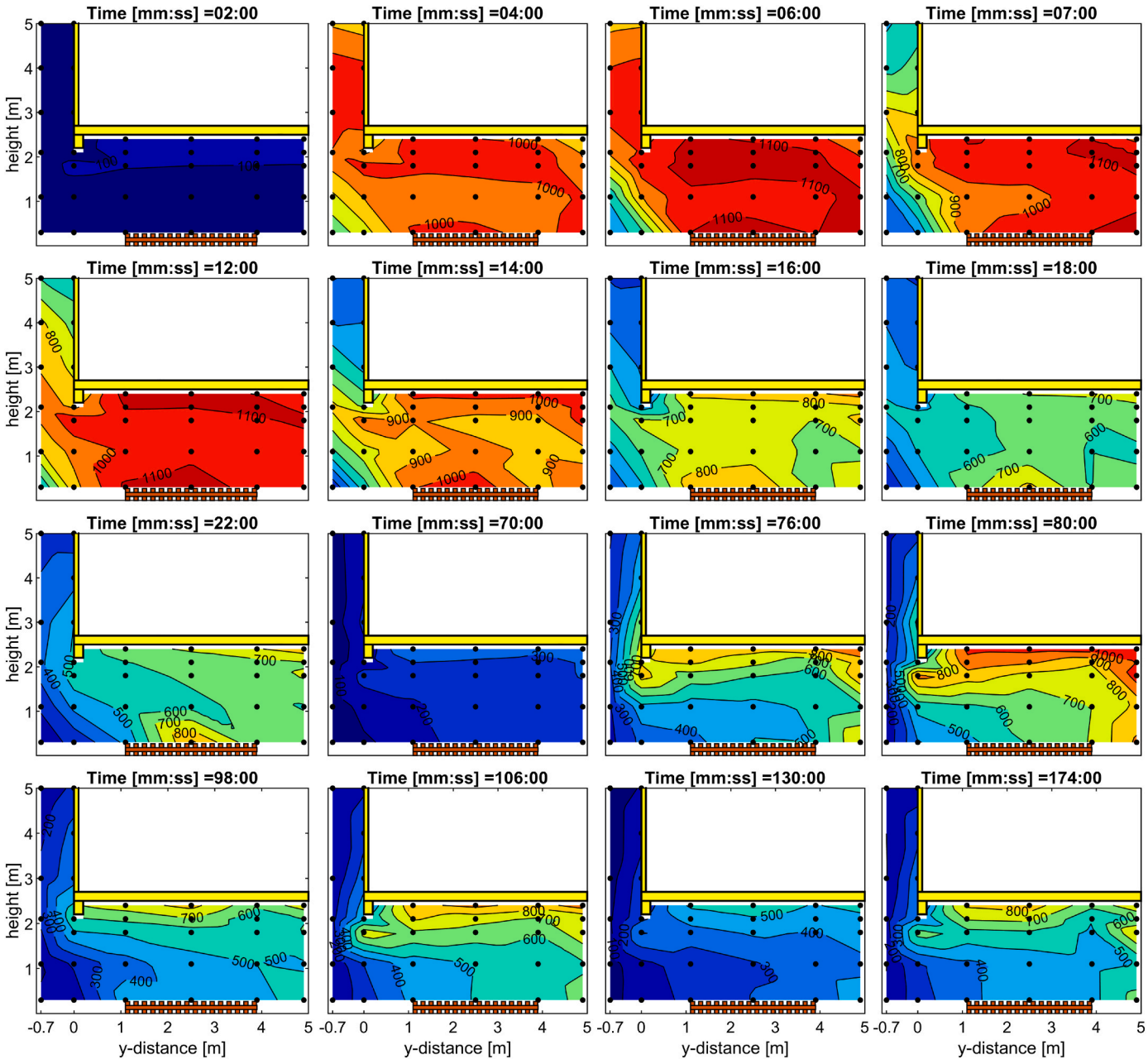

Fig. 17. Temperature map of YZ cross-section through the centre of Window 4 (X = 16.5 m).

played a role in the increased charring of the lower part of the wall. In the ceiling, however, the temperatures were the highest at the right end of the compartment, where the charring was less pronounced. This shows that temperature differences alone cannot explain the large variations in char depth.

Fig. 31 shows the burn-through below the wall and is a great example that connection details are crucial to fire safety in CLT buildings. This was caused by the lack of sealant between the wall and the bottom plank, resulting in tiny gaps for the fire to spread through. This emphasises the need for fire-rated seals between CLT elements to avoid fire spread through small gaps. Another example from this experiment was the inadequate extinguishing of the inner corner area between the ceiling and the glulam beam, which allowed smouldering combustion to continue. Ultimately, this ongoing smouldering process burned through the ceiling and caused a re-ignition which was discovered 7–8 h after termination of the experiment. A similar example of continued smouldering of CLT and a thorough discussion about this topic is given by Mitchell et al. [34].

4.3. *Self-extinguishment of flames at the CLT and second flashover*

Self-extinction of flames at the CLT wall and ceiling occurred at temperatures between 805 and 845 °C (measured by PTs) and an incident heat flux of 70–84 kW/m^2. These values are higher than typical values for self-extinction of CLT (43.6 ± 4.7 kW/m^2) [20] and higher than in #FRIC-01 (49–52 kW/m^2). The higher values can possibly be explained by the lower oxygen concentration, as a lower oxygen level requires a higher critical heat flux to sustain burning [35]. At 13 min, shortly before extinguishment of the CLT, the O_2 concentration was 13% in the outflow gas through Window 2 and 0% for Window 4, measured 0.1 m below the window soffit. Another effect that may have influenced the result is the thickness of the char layer at the point of self-extinction. Although this was not measured directly, it can be assumed that the char layer was thicker than in #FRIC-01. This is based on a faster charring

Fig. 18. Side view of external flame emerging from Window 4. Time (mm:ss) after ignition. The given times might deviate slightly (±1 s) from the exact times as the start of ignition was not recorded.

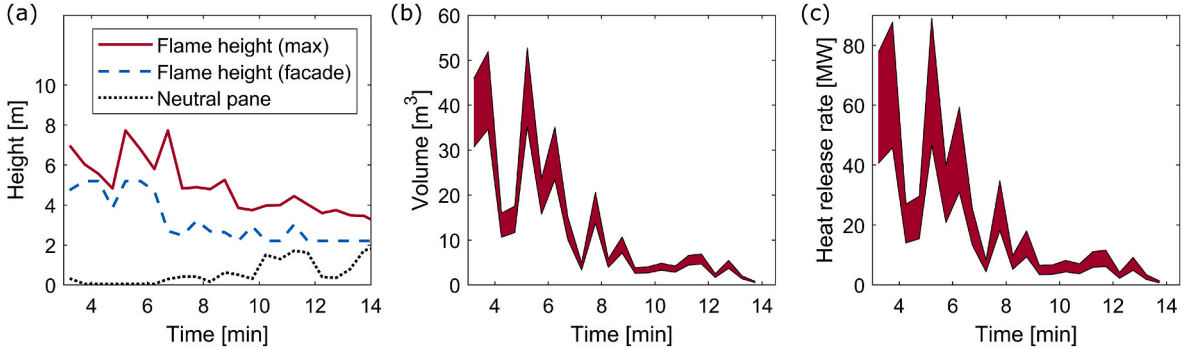

Fig. 19. Height (a), volume (b) and heat release rate (c) of the external flame from Window 4. The shaded area in (b) and (c) represent the uncertainty of the estimation.

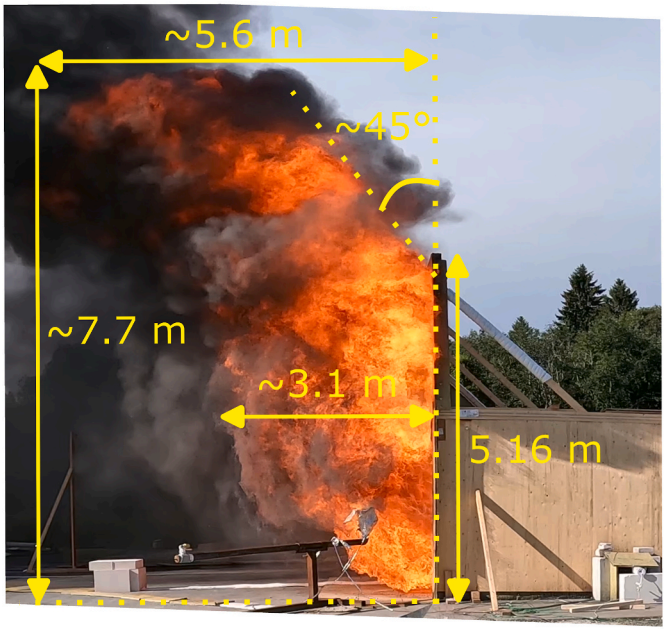

Fig. 20. Maximum external flame from Window 4. The flame height and depths are estimated based on the known facade height. Note: This flame does not represent the overall flame size but shows the absolute maximum size that occurred.

rate in #FRIC-02 but an almost identical duration of flaming combustion of the CLT compared to #FRIC-01. With a thicker insulating char layer, a higher external heat flux is needed to sustain combustion.

Shortly after the extinguishment of flames at the CLT, an apparent temperature increase was observed (Figs. 12–14). This increase was likely due to a change in the wind conditions, where the wind at this point turned to a direction coming more from the front side and to a greater extent affected the burning inside the compartment. This is shown by comparing the wind measurement at 15 and 20 min (Table 1).

Although shown earlier [14,16], this experiment is another example that a second flashover might occur after a long decay phase in compartments where no heat-resistant adhesive is implemented. Before the first flames leading to the second flashover appeared, the flaming combustion of the CLT had been out for approx. 50 min, the wood crib was completely burned out, and temperatures in the compartment had been decaying for about an hour. However, from 66 min, multiple small flames developed within 10 min to a full blaze, with peak temperatures almost reaching the same level as in the first flashover. It was observed that several flames appeared close to the growing air gaps at the bottom of the wall, see Fig. 31. The air gaps might have speeded up the charring rate around these points. Still, since flames appeared at many different locations in the ceiling and the wall approximately at the same time, it is concluded that the air gap did not significantly affect the transition to the second flashover.

An indication of the ongoing smouldering before the second flashover was the increase in CO concentration from 25 min. A similar observation was made in #FRIC-01 [9], where the CO concentration dropped significantly at the extinction of flames but then gradually increased.

In #FRIC-01 [9], delamination (or glue line integrity failure) happened, although the char front had not reached the glue line. This was concluded based on a few lamellas hanging down and several clearly detached from the layer behind but still in place. The layer behind was mostly discoloured but not charred, which proves that the first layer, in general, had not been charred through. The reason why the lamellas were loose and hanging down, but had not fallen down, can be explained by a) only part of the lamella length was detached due to the non-uniform char depth along the lamellae length, and b) a lamella not entirely charred through will have some remaining strength that prevents it from falling down or breaking into pieces.

It is believed that the delamination process in this experiment occurred similarly as in #FRIC-01. This is supported by observations where flames emerged from behind the outer lamellas, indicating an air gap between the two outer layers. In addition, the first pieces of wood falling off were seen at 70 min, when multiple flames already had appeared. However, after the second flashover, pieces of wood were falling almost continuously during the most intense burning phase.

With the delamination occurring before the exposed lamellae was charred through, two preheated surfaces with fresh timber were exposed with a small air gap in between. The two preheated surfaces were shielded from any external radiation but were heated by the gas temperature next to the CLT and the thermal wave propagating through the first CLT layer. The gas temperature was well above 400 °C at several locations when the first flames occurred before the second flashover. From the many simultaneously occurring fires around this time, it is evident that the described conditions were ideal for a fire to emerge in the gap between the two layers.

After the second flashover, the intensity and temperatures of the fire varied strongly, as seen in Figs. 9 and 12–14. The varying intensity and the compartment still burning after 175 min can be explained by three coinciding factors. 1) The burning of wood follows a natural variation in burning intensity. 2) The intermediate CLT elements were thin, only 20

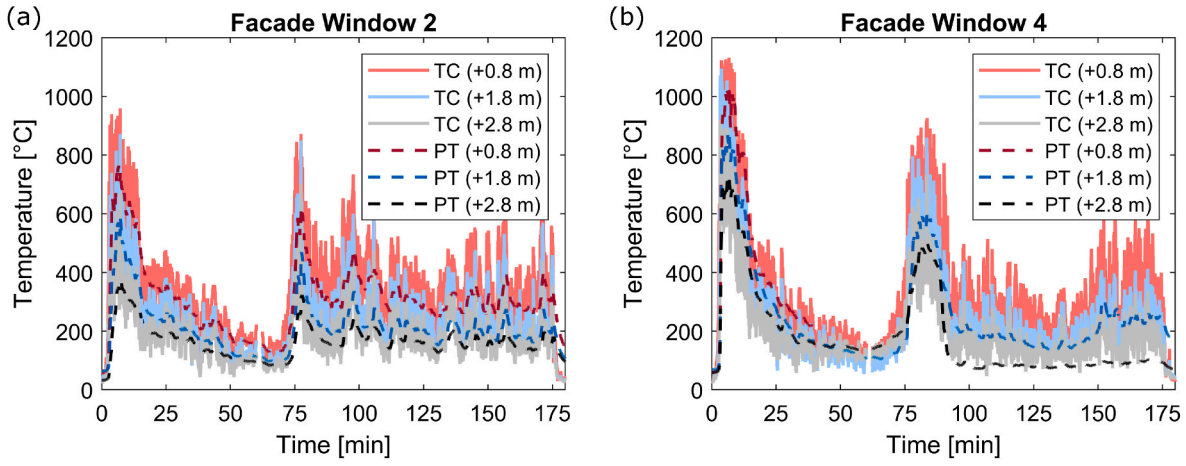

Fig. 21. Temperature measurements at the facade above Window 2 (a) and Window 4 (b). +0.8, 1.8, and 2.8 m are heights above the window soffit. The TCs are not corrected for any radiation exposure and might deviate slightly from the real gas temperature.

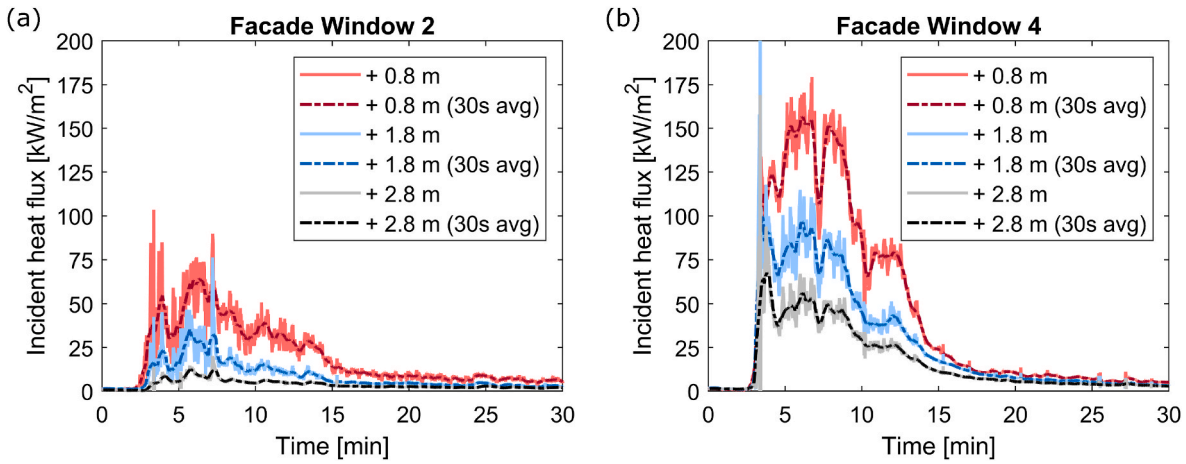

Fig. 22. Incident heat flux at the facade above Window 2 (a) and Window 4 (b). +0.8, 1.8, 2.8 m are heights above the window soffit.

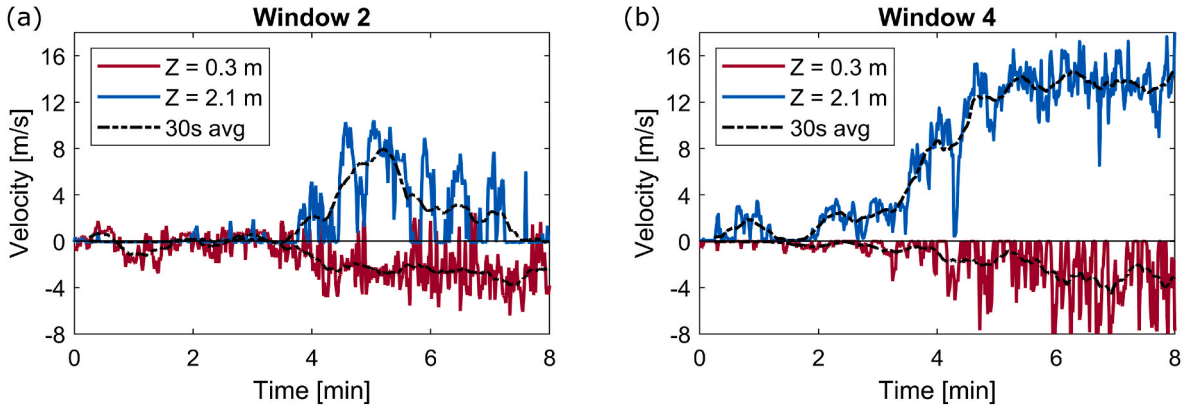

Fig. 23. Gas flow velocities inwards and outwards through Window 2 (a) and Window 4 (b). Positive values represent outward flow, and negative values inward flow.

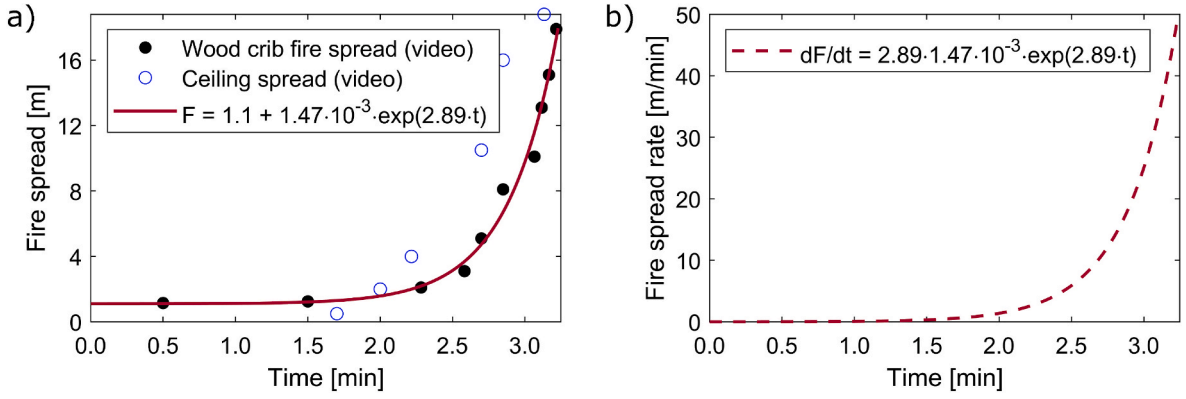

Fig. 24. (a) Fire spread across the wood crib and the ceiling. (b) Fire spread rate across the wood crib.

mm thick. 3) The adhesive of the CLT did not have sufficient resistance against glue-line integrity failure.

Firstly, part of the variation in intensity can be explained by the typical burning behaviour of wood when subjected to an external heat flux. At ignition, the wood burns with flaming combustion with a typical high charring rate. Over time a thicker and thicker char layer forms, and to sustain flaming combustion, the incident heat flux must overcome a critical value. At 120 min, the fire had its least intense period with only minor flames. The few flames present at this point appeared to be emerging from the layer behind and not from burning of the outermost CLT layer. This corresponds well with the measured incident heat fluxes of 31 kW/m^2 for the back wall and 36 kW/m^2 for the ceiling, in which both are below the critical heat flux for self-extinguishment of flames at a CLT surface [20]. The lowest incident heat fluxes were present at 128 min, although considerably more flames were present at this point than at 120 min, see Fig. 9. This again strengthens the hypothesis that the flames were coming from the fresh timber exposed due to delamination. Since the intermediate layers were only 20 mm thick, and we assume that delamination happened before the char front had reached through, the effective thickness before delamination occurred was, therefore, less

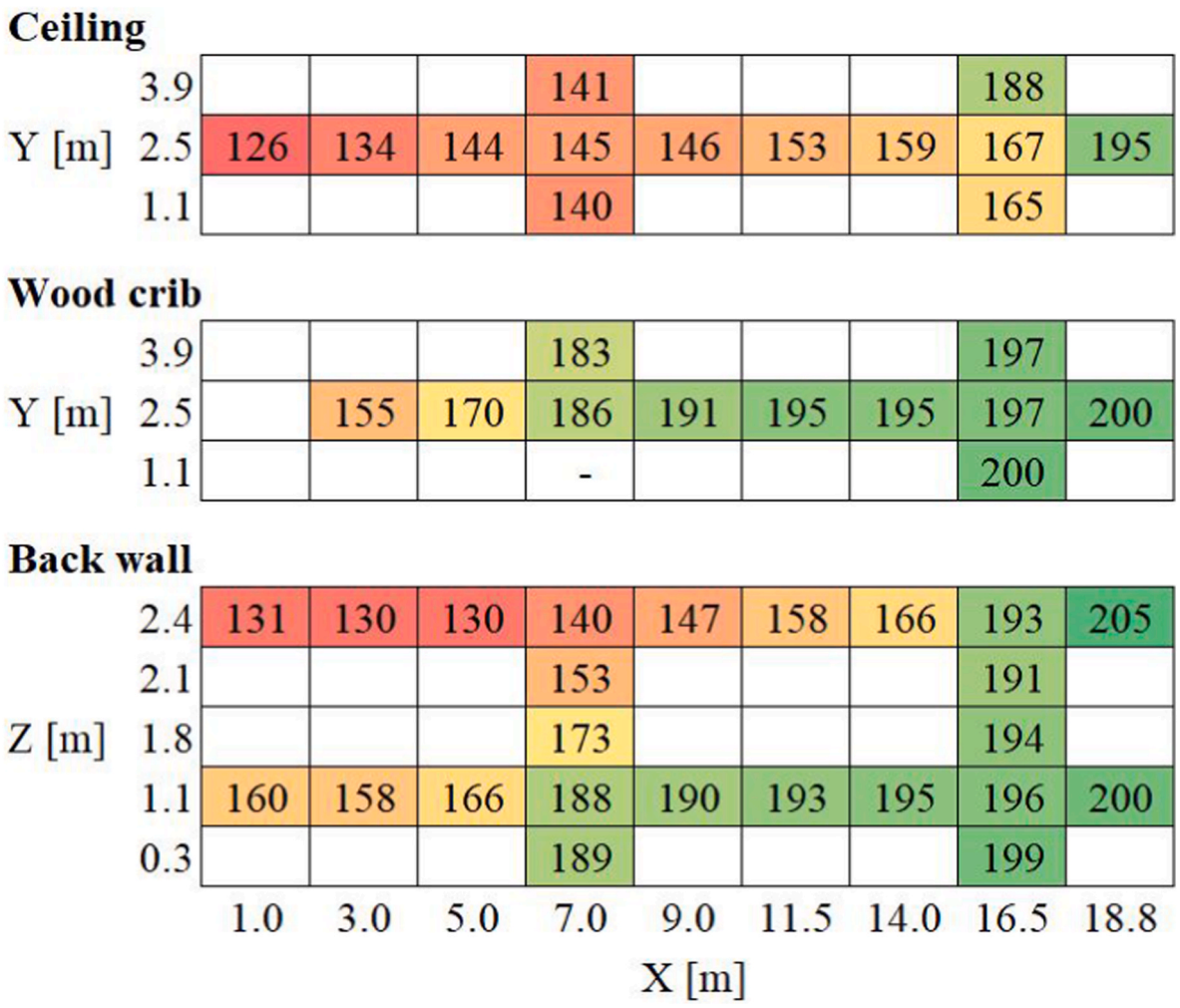

Fig. 25. Fire spread indicated by a TC temperature of 600 °C. The fire spread firstly across the ceiling and top of the wall, followed by lower parts of wall and the wood crib. Numbers are given in seconds after the start of the experiment. X, Y and Z represent the positions, as seen in Figs. 3 and 5.

than 20 mm.

Due to the uneven char depth (see Fig. 30) at the start of the second flashover (explained in Section 4.2), the time of delamination occurred over a range of times. This can be seen through the varying temperatures locally in the compartment, see Fig. 32. The peaks are shifted in time, corresponding to the later involvement of the left end of the wall to the fire. From the figure, it appears that the delamination cycle was approx. 30 min. The short time between the delaminations and the subsequent addition of fresh wood to the fire contributed to keep the compartment temperatures high. As an example, the PT temperature remained above 550 °C below the ceiling and 500 °C by the wall after the second flashover. In comparison, the temperatures next to the wall and ceiling after the first flashover were at the minimum 386 and 420 °C, respectively.

From the minimum temperatures at 128 min, the fire grew in intensity. When the fire was extinguished, at 175 min, it was at its most intense phase since 106 min. At this point, the incident heat fluxes to the wall and ceiling were 53 and 60 kW/m^2 and had a rising trend. If the fire had not been put out at this time, it seems likely that the fire intensity could have increased even more, possibly to a full third flashover.

Since the wall had been used in #FRIC-01, it is relevant to consider whether this affected the delamination process. The maximum temperature measured at the glue line in #FRIC-01 was 68 °C. Any official documentation on whether this temperature is sufficient to change the adhesive properties has not been received. However, small fires appeared randomly in both the wall and the ceiling almost simultaneously just before the second flashover. This parallel behaviour strongly indicates that the CLT wall behaved similarly to the CLT ceiling, which had not been used in #FRIC-01.

4.4. *External flames*

The external flaming in this experiment showed some characteristic behaviour. Firstly, the external flaming was highly non-symmetrical, with most of the external combustion taking place outside Window 4. The size of the external flame out of this window varied significantly during the most intense period. For longer periods, the flame reached above the facade walls, i.e., >3 *m* above the window soffit. And for short periods, the flame reached 5–6 *m* above the window soffit and would likely have reached even higher with a taller facade wall.

Based on the video analysis of the flame and the elevated incident heat fluxes measured on the facade walls, it is reasonable to claim that such large external flames as observed in this experiment pose a significant fire risk to ignite the storey above, but also likely two storeys above, in an actual building. In addition, such large flames are a threat to cause fire spread to an opposite building due to the large flame surface area and the large flame extension from the facade.

The non-symmetrical external flames were likely affected by the wind conditions. The direction of the wind was diagonally from behind the right end, see Table 1 and Fig. 2. Such conditions would create an underpressure on the front side of the compartment. It is suspected that the underpressure caused smoke and flames to be dragged mainly out of

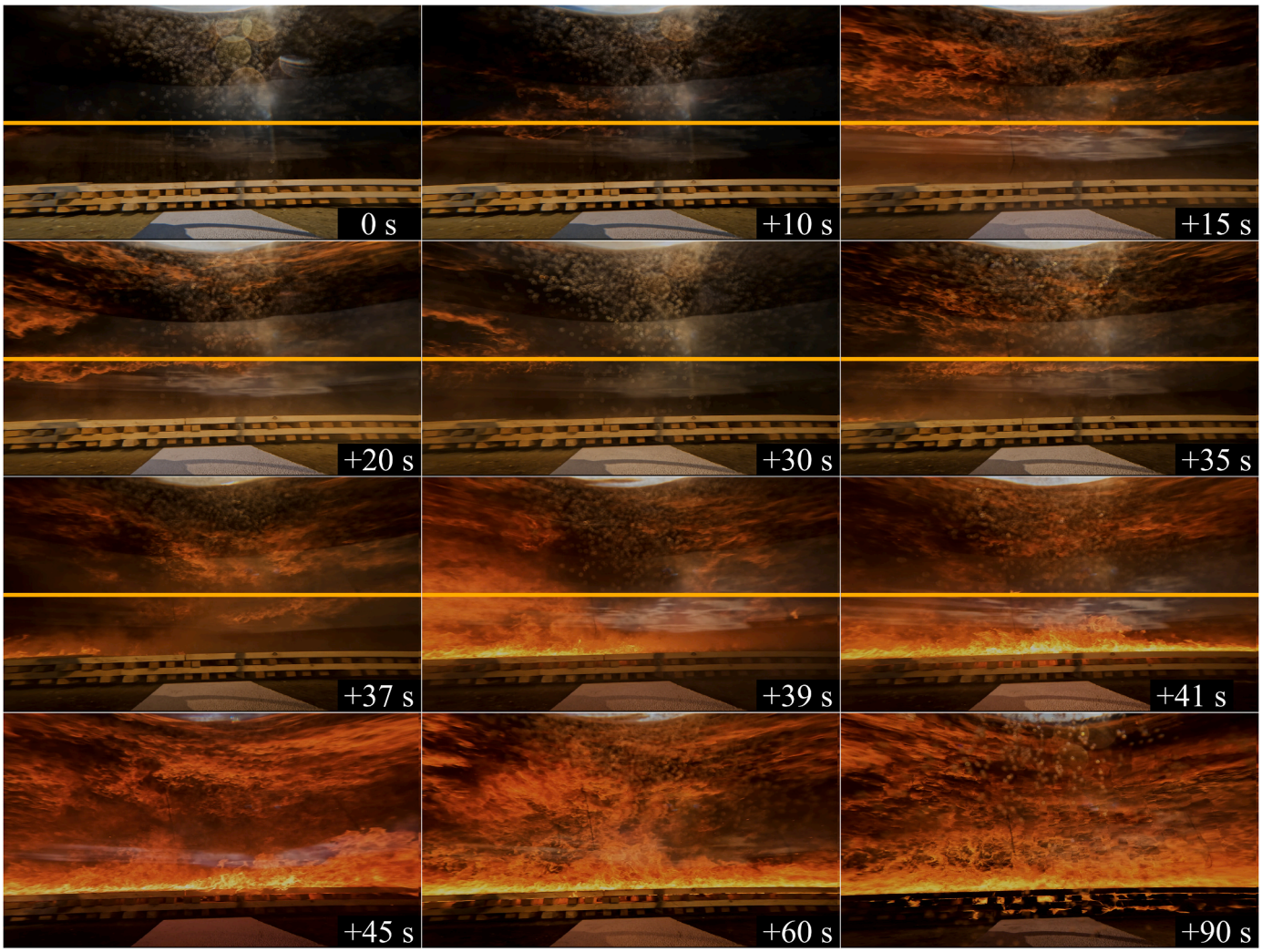

Fig. 26. The images show the fire spread sequence in the compartment. The fire spreads first across the ceiling and the upper part of the wall and then down the wall. The top layer of the wood crib ignites at about the same time the flames on the wall reach the wood crib level. The yellow line shows the top of the wall. The given time represents the number of seconds after the flame first occurs below the ceiling in this video frame. The camera was located at floor level in the centre of Window 3 inside a water-filled Pyrex column. (For interpretation of the references to colour in this figure legend, the reader is referred to the Web version of this article.)

Window 4, as the other windows were more shielded from this effect by the compartment itself. It is also likely that the largest external flames occurred due to wind gusts, which amplified this effect. From the side view of the external flame, see Fig. 18, it is evident that the flame covered the entire height at part of the window closest to the edge and that the inward flow of air was reduced through Window 4 compared to the other windows. In addition, the intense fire at this point needed a large supply of air, and since less air was supplied through Window 4, the other windows had to compensate for that loss by supplying even more air. The reduced supply of air through Window 4 caused very high and uniform temperatures in the right end of the compartment and lower temperatures in the centre of the compartment where most air was supplied (Figs. 15 and 16). The non-uniform supply of air through the windows also led to very low levels of oxygen in the right end of the compartment and indicates that part of the compartment was strongly under-ventilated during the most intense fire, despite the large window openings. It is likely that this non-symmetrical behaviour of the external flame could only occur under specific wind conditions. However, it can be stated that fire safety engineering methods to determine external fire plume heights, such as the Law-model in the Eurocodes [6], do not consider such an extent of non-uniformity along the facade openings and do not include the contribution of combustible gases from the CLT to the total HRR.

The estimated HRR for the maximum external flames from Window 4 was 66 ± 20 MW, which does not align with a total HRR of 73 MW, see Fig. 34, as this would mean that two-thirds or more of the combustible gases were burnt outside. It is acknowledged that the estimation of the external flame involved significant uncertainties, both through the determination of the flame volume and by the conversion from volume to HRR. In addition, the method to determine the heat release of external combustion was developed based on smaller flames. Still, the estimated HRR of the external flame indicates that the total HRR is estimated too low, at least for some period. A factor that significantly influences the HRR is the combustion efficiency. This was set to 0.8, but given the high temperatures in the compartment and the strong re-radiation between the crib, the wall and the ceiling, it is not unlikely that the combustion efficiency could be higher than 0.8. Given that the combustion efficiency is correct, the HRR from the wood crib is considered to be quite accurate. However, the HRR from the CLT wall and ceiling is based on only three measurements each, where the average value of those is used to estimate the HRR from the CLT. Since there was quite a large difference between the minimum (1.90 mm/min) and maximum (3.28 mm/min) charring rate, it is not unlikely that the calculated average value is lower than the actual average value. Assuming a combustion efficiency of 0.9 instead of 0.8 and an average charring rate of 3 mm/min instead of 2.64 and 2.71 mm/min, the estimated total HRR ends up being 92.5 MW, almost 20

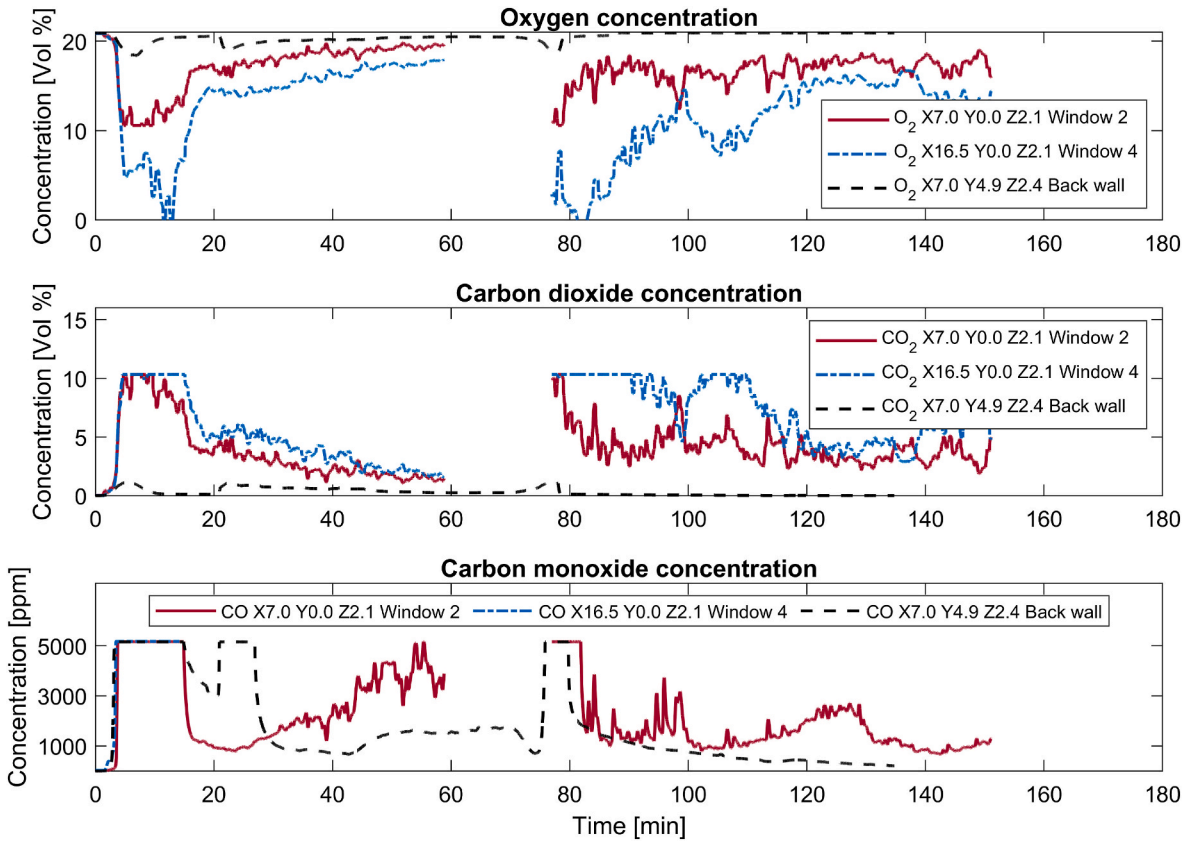

Fig. 27. O_2, CO_2 and CO concentrations of the compartment.

Table 3
Charring rates CLT ceiling.

	Time to 300 °C [min]						Charring rate [mm/min]					
	0 mm	10 mm	20 mm	30 mm	40 mm	97[a)] mm	0–10 mm	10–20 mm	20–30 mm	30–40 mm	40-97[a)] mm	0-97[a)] mm
X4.7	2.0	5.6	13.6	38.3	81.3	175	2.74	1.25	0.40	0.23	0.61	0.56
X9.5	2.3	5.3	10.9	36.6	79.6	175	3.28	1.80	0.39	0.23	0.50	0.56
X14.3	2.5	7.7	16.0	39.2	89.9	175	1.90	1.21	0.43	0.20	0.44	0.56
Avg	2.2	6.2	13.5	38.0	83.6	175	2.64	1.42	0.41	0.22	0.52	0.56

[a] 97 mm is the average final char depth in the ceiling.

Table 4
Charring rates CLT back wall.

	Time to 300 °C [min]						Charring rate [mm/min]					
	0 mm	10 mm	20 mm	30 mm	40 mm	104[a)] mm	0–10 mm	10–20 mm	20–30 mm	30–40 mm	40-104[a)] mm	0-104[a)] mm
X4.7	2.6	7.2	22.4	–	79.3	175	2.17	0.66	0.35	0.35	0.67	0.60
X9.5	2.9	6.5	13.1	–	–	175	2.82	1.50	–	–	–	0.60
X14.3	3.3	6.5	13.6	43.9	77.4	175	3.14	1.41	0.33	0.30	0.66	0.61
Avg	2.9	6.7	13.4	43.9	78.4	175	2.71	1.46[b)]	0.34	0.32	0.67	0.60

[a] 104 mm is the average final char depth in the back wall. b) The value of 0.66 mm/min is not included in the average, as it appears to be an outlier.

MW higher than the original estimation. This underlines that with minor adjustments in the parameters affecting the HRR, it does not seem unlikely that the lower HRR estimation (46 MW) of the external flame might be correct. Determination of the HRR in large-scale experiments is challenging, and a certain uncertainty must be expected.

It is well known that the size of external flames tends to increase with exposed CLT [14]. However, this problem has mainly been attributed to compartments with small window openings, which typically result in ventilation-controlled fires [36]. This experiment is an example that large external flames might also occur when having large ventilation openings. However, to know how severe the external flames were in this experiment, it is relevant to compare them against other CLT experiments that experienced large external flames. In Fig. 35, the PT measurements of the facade above Window 4 are compared to Test 2 of the CLT experiments of Sjöström et al. [37]. The experiment had an area of 48 m^2, an opening factor of 0.062 $m^{1/2}$, a fuel load density of 560 MJ/m^2 and both the ceiling and two walls exposed. The PTs were, as in this experiment, installed flush with the facade wall (see Fig. 36).

As the locations of the PTs were not at the same height above the openings, a detailed comparison is not possible. Nevertheless, the

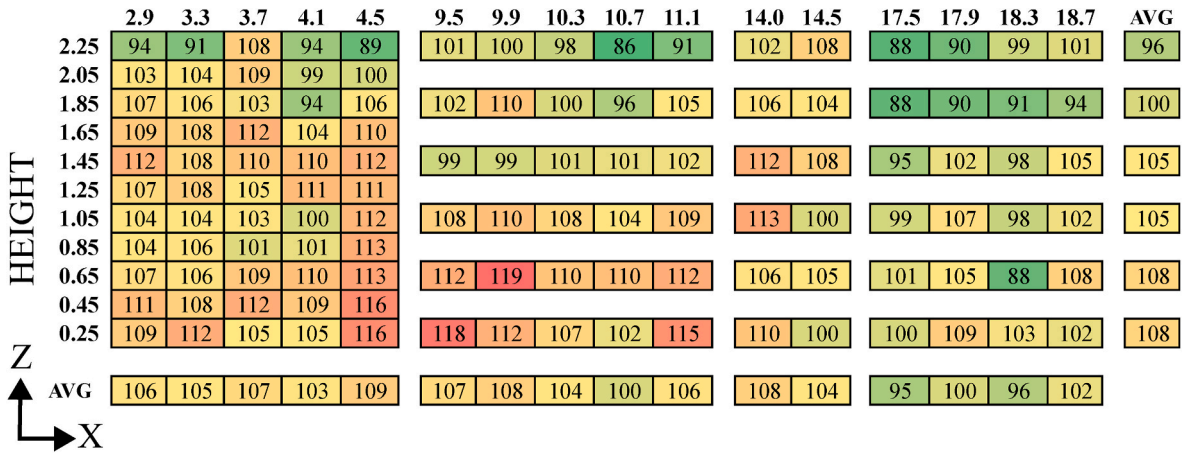

HEIGHT	2.9	3.3	3.7	4.1	4.5	9.5	9.9	10.3	10.7	11.1	14.0	14.5	17.5	17.9	18.3	18.7	AVG
2.25	94	91	108	94	89	101	100	98	86	91	102	108	88	90	99	101	96
2.05	103	104	109	99	100												
1.85	107	106	103	94	106	102	110	100	96	105	106	104	88	90	91	94	100
1.65	109	108	112	104	110												
1.45	112	108	110	110	112	99	99	101	101	102	112	108	95	102	98	105	105
1.25	107	108	105	111	111												
1.05	104	104	103	100	112	108	110	108	104	109	113	100	99	107	98	102	105
0.85	104	106	101	101	113												
0.65	107	106	109	110	113	112	119	110	110	112	106	105	101	105	88	108	108
0.45	111	108	112	109	116												
0.25	109	112	105	105	116	118	112	107	102	115	110	100	100	109	103	102	108
AVG	106	105	107	103	109	107	108	104	100	106	108	104	95	100	96	102	

Fig. 28. Final char depth [mm] measurements of CLT wall elements. X and Z represent compartment coordinates. Dark green marks the lowest char depths, and dark red marks the largest. (For interpretation of the references to colour in this figure legend, the reader is referred to the Web version of this article.)

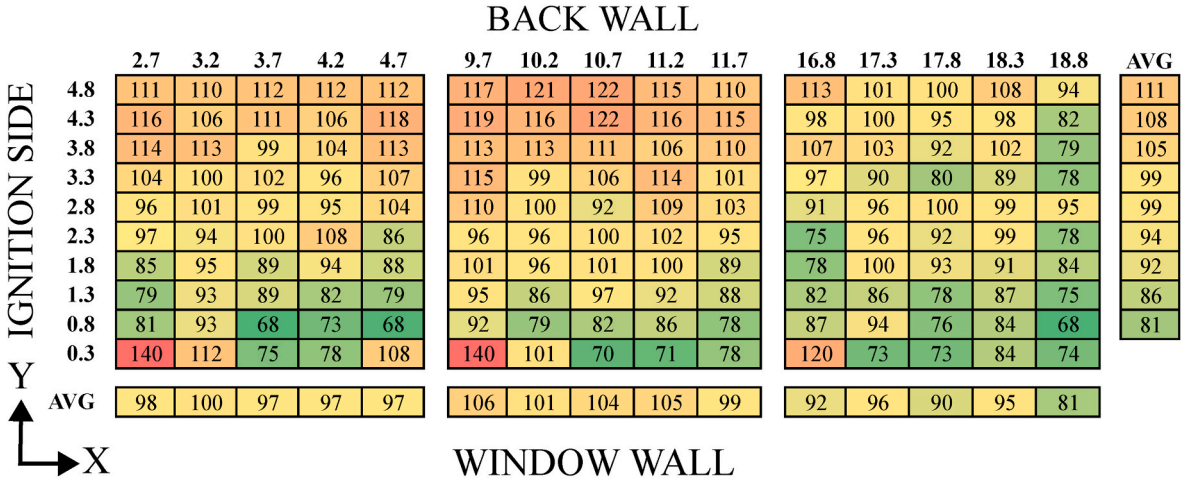

IGNITION SIDE	2.7	3.2	3.7	4.2	4.7	9.7	10.2	10.7	11.2	11.7	16.8	17.3	17.8	18.3	18.8	AVG
4.8	111	110	112	112	112	117	121	122	115	110	113	101	100	108	94	111
4.3	116	106	111	106	118	119	116	122	116	115	98	100	95	98	82	108
3.8	114	113	99	104	113	113	113	111	106	110	107	103	92	102	79	105
3.3	104	100	102	96	107	115	99	106	114	101	97	90	80	89	78	99
2.8	96	101	99	95	104	110	100	92	109	103	91	96	100	99	95	99
2.3	97	94	100	108	86	96	96	100	102	95	75	96	92	99	78	94
1.8	85	95	89	94	88	101	96	101	100	89	78	100	93	91	84	92
1.3	79	93	89	82	79	95	86	97	92	88	82	86	78	87	75	86
0.8	81	93	68	73	68	92	79	82	86	78	87	94	76	84	68	81
0.3	140	112	75	78	108	140	101	70	71	78	120	73	73	84	74	
AVG	98	100	97	97	97	106	101	104	105	99	92	96	90	95	81	

Fig. 29. Final char depth [mm] measurements of CLT ceiling elements. X and Y represent compartment coordinates. The measurements at 0.3 *m* height were not included in the average. Dark green marks the lowest char depths, and dark red marks the largest. (For interpretation of the references to colour in this figure legend, the reader is referred to the Web version of this article.)

temperatures were in about the same range but slightly lower in this experiment. In addition, the duration of the exposure was about three times longer in Test 2. Summarised, the facade exposure in this experiment was for a short period, almost as severe as Test 2, which had a 60% higher fuel load density and was a strongly under-ventilated fire.

4.5. Comparison between #FRIC-01 (exposed ceiling) and #FRIC-02 (exposed ceiling and wall)

The fire developed completely differently in #FRIC-01 and #FRIC-02. These differences can be explained by the three changes in the experimental setup: 1) Exposed CLT on the back wall. 2) Different wind conditions. 3) A different ignition source, as detailed below.

The differences in the ignition source are highlighted in Table 6 and shown in Fig. 35. The increase in the heptane amount was because the wood crib fire in #FRIC-01 almost extinguished after 4 min when the heptane fire burned out. We were afraid that the wood crib fire in #FRIC-02 could extinguish completely if no changes were made to the ignition source. Hence, to avoid the risk of extinguishment of the wood crib fire in #FRIC-02, the ignition method was changed to ensure the wood crib fire was well established when the heptane fire burned out.

In #FRIC-01, the initial heptane and wood crib fire did not ignite the ceiling, and the ceiling was ignited first after 32.5 min when the CLT ceiling had been heated sufficiently to auto-ignite. By changing the ignition source in #FRIC-02, the heptane fuel surface increased by 40%, and the setup also exposed a larger portion of the wood crib to the fire. This change turned out to be sufficient to ignite the ceiling early.

From the point the ceiling was ignited in the two experiments, the fire development was completely different. In #FRIC-01, the ceiling had been preheated for about half an hour, and the ignition of it caused a rapid flash fire over a large area of the ceiling. In #FRIC-02, the ceiling had not been preheated, and the fire spread across the ceiling developed slower. While the ceiling fire in #FRIC-01 retracted quickly, the ceiling fire in #FRIC-02 continued to spread and developed into a full flashover 1.5 min after the ceiling was ignited. In #FRIC-01, on the other hand, the fire spread across the room in 13 min, where the leading edge of the fire travelled back and forth in three flashing waves before flashover was reached after the fourth wave. This difference is believed to be directly linked to the exposed back wall in this experiment. From video analysis, and also shown in Fig. 26, it is evident that the wall worked as a bridge between the ceiling and the wood crib. The CLT wall contributed to emissions of combustible gases before ignition and after ignition to increased radiation to the wood crib and the ceiling. This re-radiation between three burning surfaces was here sufficient to maintain burning in all of them, and no retraction of the flames was observed.

That the top of the wall ignited about the same time as the ceiling

Fig. 30. Visualization of non-uniform charring for one CLT ceiling element based on a photo. Black is the 3rd layer, yellow is the 4th, and red is the 5th layer. The holes at the right and left lower corners of the window side were caused by smouldering and reignition after the end of the experiment, as this part was hard to reach with water due to safety precautions. (For interpretation of the references to colour in this figure legend, the reader is referred to the Web version of this article.)

with flame spread downwards was expected based on the measured heat fluxes at the wall in #FRIC-01, which was 10–40 kW/m^2 between the 1st and 2nd flashing wave. This level is well above what is needed for piloted ignition of a wooden surface [38].

In addition to the increased spread rate in this experiment, the temperatures, the HRR and the external flames were also higher. The temperatures were during the most intense period 1010–1172 °C in the whole compartment, while in #FRIC-01, they were 785–1038 °C. The more extreme temperatures were caused by a higher HRR, which was estimated to be 32 MW (78%) higher at maximum for #FRIC-02, of which 13 MW was directly caused by the combustion of the CLT wall. The comparison indicates that the contribution of the exposed wall resulted in an increased combustion rate of the wood crib and the CLT ceiling. The maximum HRR of the wood crib was determined to be 15 MW (75%) higher in this experiment. From these 15 MW, 5 MW was due to the higher HRR per unit length caused by higher temperatures and more considerable heat fluxes towards the wood crib [39]. The remaining 10 MW was due to faster fire spread across the wood crib, which caused a larger part of the crib to burn simultaneously at maximum HRR per unit length.

The average charring rates in this experiment were 21% and 28% faster than in #FRIC-01 for 0–10 mm and 10–20 mm depth, respectively. This increase corresponds to an estimated HRR increase for the ceiling of 3.5 MW.

The external flames were highly non-symmetrical in this experiment, whereas in #FRIC-01, they were more symmetrical. This was likely caused by different wind conditions. In #FRIC-01, there was no measurement of the wind, but the smoke was going almost straight up, indicating a very low wind velocity. In #FRIC-02, the wind was coming diagonally from behind, and smoke and flames were going away from the compartment. Despite relatively low winds, the wind conditions in #FRIC-02 are still expected to have caused an underpressure outside of Window 4, leading to the particularly large external flames from this window, as explained in Section 4.4.

The extinction of flames at the CLT occurred in both experiments but at a higher incident heat flux in #FRIC-02 (see Section 4.3). The following decay phase was nearly linear in both experiments, with an average temperature reduction of 7.1 °C/min in #FRIC-01 and 5.7 °C/min in this experiment. The 20% slower decay rate was likely related to the re-radiation between the wall and the ceiling and more heat stored in the CLT wall than in the gypsum boards. After 65 min in #FRIC-02, the wood crib was completely consumed. The decay phase seemed to follow the behaviour of #FRIC-01, in which temperatures were continuously decaying until ambient conditions were reached, with no re-ignition. However, despite using the same CLT materials and variable fuel load, #FRIC-01 did not exhibit a re-ignition or second flashover, while #FRIC-02 did. This difference was likely due to the higher gas temperature in #FRIC-02 when delamination occurred, 430–445 °C in #FRIC-02 vs. approx. 220 °C in #FRIC-01. Furthermore, the fact that delamination in #FRIC-02 occurred simultaneously in multiple locations certainly contributed to the transition of larger flames and, eventually, the second flashover.

5. Conclusion

- The article describes the second of two compartment fire experiments where the aim was to study the effect of exposed CLT, ventilation conditions and room geometry on fire spread and fire dynamics. The setup was designed as a 95 m^2 open-plan compartment, and this is, to our knowledge, the largest experiment to date

Fig. 31. The fire burned through the intersection between the back wall and the bottom plank at approximately 60 min. The image is taken at a later point when the gap had become larger. The lack of a fire sealant between the bottom plank and the CLT wall enabled this and highlights that connection details are crucial to fire safety.

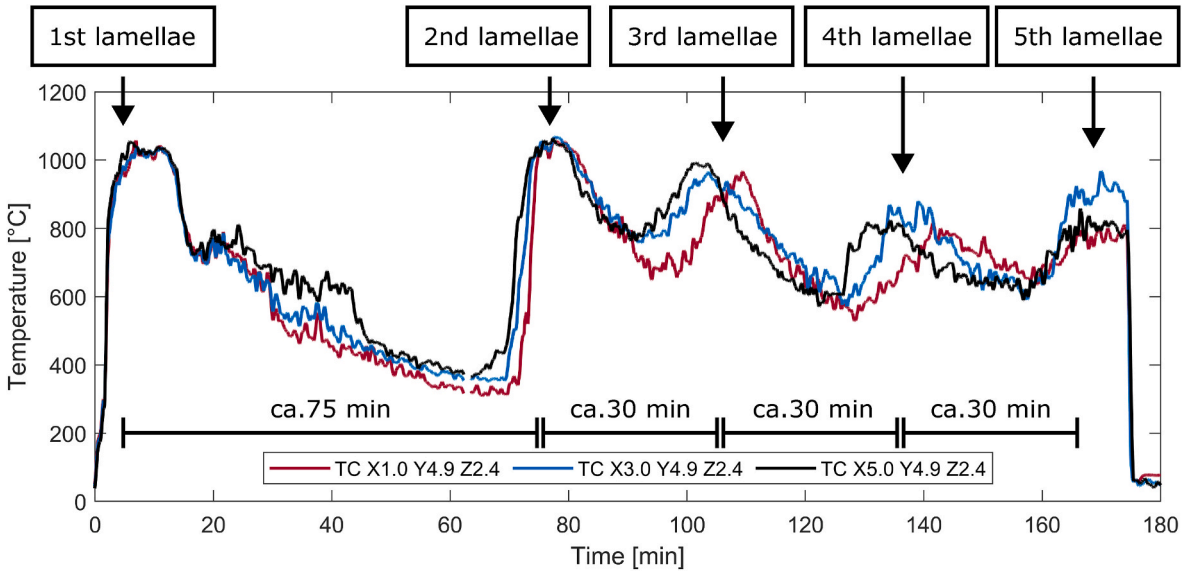

Fig. 32. Temperature of three TCs located next to the back wall. The peaks correspond to the burning of the different layers in the CLT wall.

Table 5
Estimated time for the char front to reach the different layers, based on a charring rate of 0.52 mm/min for the ceiling (Table 3) and 0.67 mm/min for the back wall (Table 4).

	Estimated time [min] for char front to reach			
	2nd layer (40 mm)	3rd layer (60 mm)	4th layer (80 mm)	5th layer (100 mm)
Ceiling	76	114	153	191
Wall	76	106	136	166

with both an exposed CLT wall and ceiling. The fire spread across the room in less than 3.5 min from ignition (5.5 m/min) and in 1.5 min from ignition of the ceiling (11.7 m/min), which is significantly faster than most values found in the literature. The fast fire spread also led to a fire growth rate considerably faster than the fastest fire growth rate in Eurocode 1.

- The accelerating flame spread rate indicates that significantly larger compartments would not necessarily take significantly more time to ignite.
- During the most intense burning phase of the fire, large asymmetrical external flames were observed. The flames were particularly large from one window and reached 3–6 m above the window soffit for several minutes after flashover. This result highlights that large external flames might also occur in compartments with large window openings.
- After an intense burning phase, the flames at the CLT extinguished, and the wood crib burned out. However, 60 min after the extinction of flames at the CLT, a second flashover occurred. The fire varied in intensity but burned with temperatures up to 800 °C when manually extinguished after 3 h. The ongoing fire resulted from the thin (20 mm) intermediate layers in the CLT and the use of an adhesive that resulted in glue-line integrity failure.
- The charring of the CLT was strongly non-uniform, with an increasing char depth of the ceiling from the window opening to the back wall and increased charring of the wall compared to the ceiling.
- Self-extinction of flames at the CLT was observed at temperatures 805–845 °C and incident heat flux 70–84 kW/m^2. This is higher than reported earlier and is assumed to be caused by the low oxygen content and thick char layer.

These results should be considered together with the results of #FRIC-01 [9] for the complete picture of the research and background information. From comparisons between #FRIC-01 (exposed ceiling) and #FRIC-02 (exposed ceiling and wall), the following is concluded.

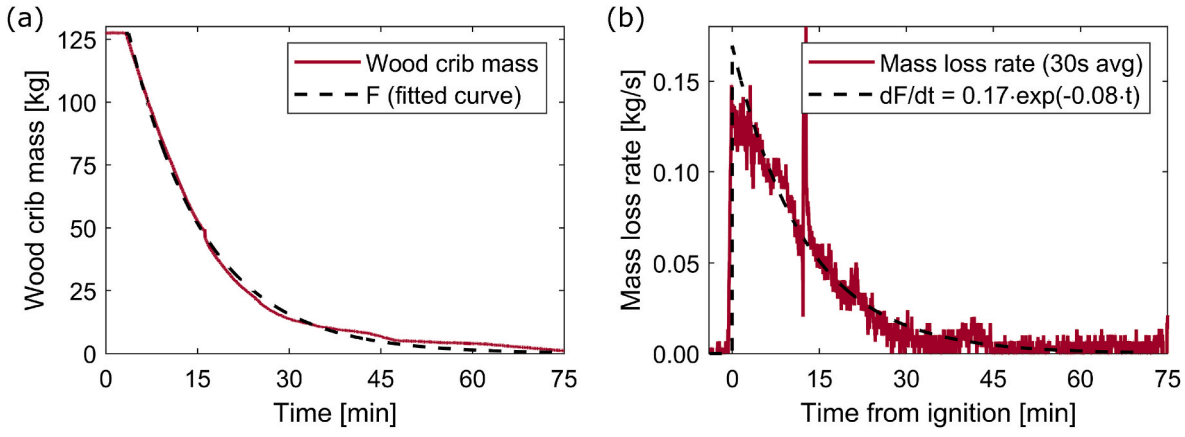

Fig. 33. (a) Mass loss of the small wood crib (1.0 m × 2.8 m) put on a scale. (b) Mass loss rate of the small wood crib.

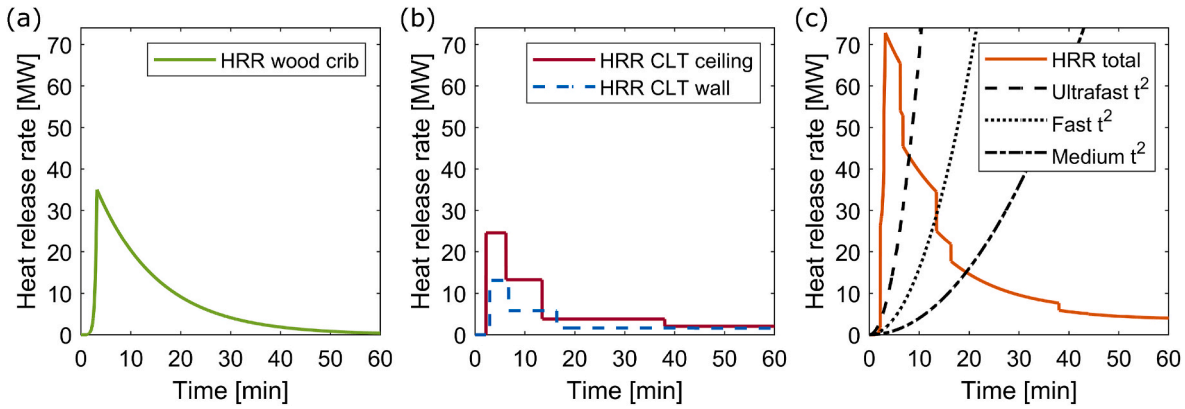

Fig. 34. Heat release rate of the wood crib (a), CLT (b) and total (c). The total HRR of the experiment is compared against the medium, fast and ultrafast fire growth rates [6].

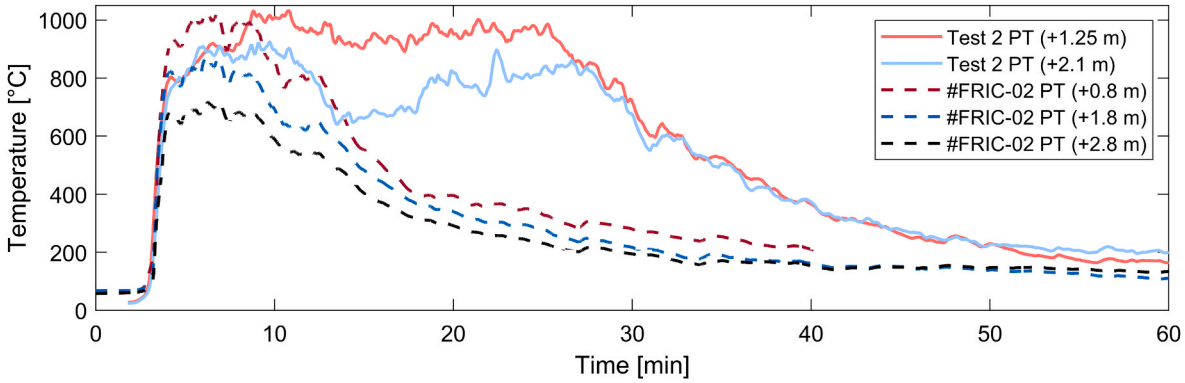

Fig. 35. Comparison of PT temperatures above Window 4 to Test 2 of Sjöström et al. [37]. The x-axis of Test 2 is shifted +1.8 min to synchronise the times for easier comparison.

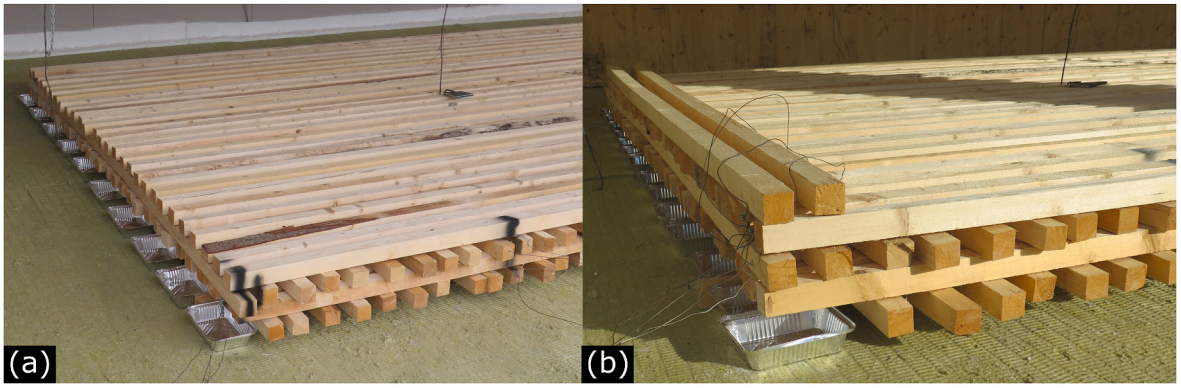

Fig. 36. Comparison of ignition method of #FRIC-01 (a) and #FRIC-02 (b). The wires shown in (b) are thermocouples from different loggers to synchronise the data.

Table 6
Differences in ignition source between #FRIC-01 and #FRIC-02.

	#FRIC-01	#FRIC-02
No. Of heptane trays	10	14
Heptane amount in each tray	0.5 L	0.7 L
Total amount of heptane	5.0 L	9.8 L
Rotation of trays	0°	90°
Part of tray below the wood crib	5 cm	15 cm

- Despite minor changes in the ignition source, the comparison indicates that the presence of an exposed wall can significantly accelerate the fire development.
- In #FRIC-02, the fire spread rate was faster, and temperatures, charring rates, heat release rates and external flames were higher.
- In #FRIC-02, a second flashover and subsequent fluctuations of fire intensity occurred, while #FRIC-01 did not exhibit a secondary flashover. This was likely caused by the increased fire exposure due to the additional fuel by the wall and increased HRR from the wood crib and CLT ceiling. This combination caused a higher gas temperature next to the CLT when delamination occurred, sufficient to ignite the fresh wood of the second layer.

Sample CRediT author statement

Andreas Sæter Bøe: Conceptualization, Methodology, Investigation, Formal Analysis, Data Curation, Writing - Original Draft, Writing - Review & Editing, Visualization.

Kathinka Leikanger Friquin: Conceptualization, Methodology, Writing - Review & Editing.

Daniel Brandon: Conceptualization, Methodology, Writing - Review & Editing.

Anne Steen-Hansen: Conceptualization, Writing - Review & Editing.

Ivar S. Ertesvåg: Conceptualization, Writing - Review & Editing.

Declaration of competing interest

The authors declare that they have no known competing financial interests or personal relationships that could have appeared to influence the work reported in this paper.

Data availability

Data will be made available on request.

Acknowledgement

The experiments were conducted at RISE Fire Research in Norway as part of the Fire Research and Innovation Centre (FRIC) (www.fric.no). The authors gratefully acknowledge the financial support by the Research Council of Norway through the program BRANNSIKKERHET, project number 294649, and by partners of the research centre FRIC. A special thanks to the FRIC partners Stora Enso, Rockwool, Hunton, and to Saint-Gobain AS and Byggmakker Handel AS for providing building materials. The authors also thank Panos Kotsovinos and David Barber at ARUP, David Lange and Juan P. Hidalgo at The University of Queensland, and Johan Sjöström at RISE for valuable discussions in the planning phase of the experiments. We would also like to thank Johan Sjöström for access to temperature data for comparison.

Appendix A. Supplementary data

Supplementary data to this article can be found online at https://doi.org/10.1016/j.firesaf.2023.103986.

References

[1] G. Ronquillo, D. Hopkin, M. Spearpoint, Review of large-scale fire tests on cross-laminated timber, J. Fire Sci. 39 (5) (2021) 327–369, https://doi.org/10.1177/07349041211034460.

[2] J. Liu, E.C. Fischer, Review of large-scale CLT compartment fire tests, Construct. Build. Mater. 318 (2022), 126099, https://doi.org/10.1016/j.conbuildmat.2021.126099.

[3] H. Mitchell, P. Kotsovinos, F. Richter, D. Thomson, D. Barber, G. Rein, Review of fire experiments in mass timber compartments: current understanding, limitations, and research gaps, Fire Mater. 47 (4) (2023) 415–432, https://doi.org/10.1002/fam.3121.

[4] P. Kotsovinos, et al., Fire dynamics inside a large and open-plan compartment with exposed timber ceiling and columns: CodeRed #01, Fire Mater. 47 (4) (2023) 542–568, https://doi.org/10.1002/fam.3049.

[5] P. Kotsovinos, et al., Impact of ventilation on the fire dynamics of an open-plan compartment with exposed timber ceiling and columns: CodeRed #02, Fire Mater. 47 (4) (2023) 569–596, https://doi.org/10.1002/fam.3082.

[6] EN 1991 1-2 (2002) Eurocode 1: Actions on Structures - Part 1-2: General Actions - Actions on Structures Exposed to Fire, CEN, Brussels, Belgium, 2002.

[7] E. Rackauskaite, et al., Fire experiment inside a very large and open-plan compartment: x-ONE, Fire Technol. 58 (2022) 905–939, https://doi.org/10.1007/s10694-021-01162-6.

[8] M. Heidari, et al., Fire experiments inside a very large and open-plan compartment: x-TWO, in: Presented at the Proceedings of the 11th International Conference on Structures in Fire (SiF2020), The University of Queensland, Brisbane, Australia, 2020.

[9] A.S. Bøe, K.L. Friquin, D. Brandon, A. Steen-Hansen, I.S. Ertesvåg, Fire spread in a large compartment with exposed cross-laminated timber and open ventilation conditions: #FRIC-01 - exposed ceiling, Fire Saf. J. (2023), 103869, https://doi.org/10.1016/j.firesaf.2023.103869.

[10] A. Nadjai, et al., Large scale fire test: the development of a travelling fire in open ventilation conditions and its influence on the surrounding steel structure, Fire Saf. J. 130 (2022), 103575, https://doi.org/10.1016/j.firesaf.2022.103575, 2022/06/01/.

[11] J.P. Hidalgo, et al., The Malveira fire test: full-scale demonstration of fire modes in open-plan compartments, Fire Saf. J. 108 (2019), https://doi.org/10.1016/j.firesaf.2019.102827.

[12] R.M. Hadden, et al., Effects of exposed cross laminated timber on compartment fire dynamics, Fire Saf. J. 91 (2017) 480–489, https://doi.org/10.1016/j.firesaf.2017.03.074.

[13] X. Li, X. Zhang, G. Hadjisophocleous, C. McGregor, Experimental study of combustible and non-combustible construction in a natural fire, Fire Technol. 51 (6) (2015) 1447–1474, https://doi.org/10.1007/s10694-014-0407-4.

[14] J. Su, P.-S. Lafrance, M.S. Hoehler, M.F. Bundy, Fire Safety Challenges of Tall Wood Buildings–phase 2: Task 3-Cross Laminated Timber Compartment Fire Tests. Report No. FPRF-2018-01-REV, NFPA (National Fire Protection Association), Quincy, Massachusetts, USA, 2018. March 28, 2023. [Online], https://tsapps.nist.gov/publication/get_pdf.cfm?pub_id=925297.

[15] D. Brandon, J. Sjöström, A. Temple, E. Hallberg, F. Kahl, RISE report - final Project Report - fire Safe implementation of visible mass timber in tall buildings - compartment fire testing (2021:40), RISE Fire Res, 2021, p. 40 [Online], http://urn.kb.se/resolve?urn=urn:nbn:se:ri:diva-58153. RISE Report 2021.

[16] A.R. Medina Hevia, Fire Resistance of Partially Protected Cross-Laminated Timber Rooms, Carleton University, Ottawa, Ontario, 2014. Master thesis.

[17] C. Dagenais, L. Ranger, N. Benichou, J. Su, "Improved fire performance of cross-laminated timber," presented at the World Conference on Timber Engineering, Santiago, Chile (2021) 9–12. August.

[18] D. Hopkin, et al., Large-scale enclosure fire experiments adopting CLT slabs with different types of polyurethane adhesives: genesis and preliminary findings, Fire 5 (2) (2022), https://doi.org/10.3390/fire5020039.

[19] R. Emberley, et al., Description of small and large-scale cross laminated timber fire tests, Fire Saf. J. 91 (2017) 327–335, https://doi.org/10.1016/j.firesaf.2017.03.024.

[20] R. Emberley, T. Do, J. Yim, J.L. Torero, Critical heat flux and mass loss rate for extinction of flaming combustion of timber, Fire Saf. J. 91 (2017) 252–258, https://doi.org/10.1016/j.firesaf.2017.03.008.

[21] R. Crielaard, J.-W. van de Kuilen, K. Terwel, G. Ravenshorst, P. Steenbakkers, Self-extinguishment of cross-laminated timber, Fire Saf. J. 105 (2019) 244–260, https://doi.org/10.1016/j.firesaf.2019.01.008, 2019/04/01/.

[22] EN 520:2004+A1:2009, Gypsum Plasterboards - Definitions, Requirements and Test Methods, CEN, Brussels, Belgium, 2004.

[23] EN 1995-1-2 (Eurocode 5): Design of Timber Structures - Part 1-2: General - Structural Fire Design, CEN, Brussels, Belgium, 2004.

[24] U. Wickström, Temperature Calculation in Fire Safety Engineering, Springer, 2016.

[25] B.J. McCaffrey, G. Heskestad, A robust bidirectional low-velocity probe for flame and fire application, Combust. Flame 26 (1976) 125–127, https://doi.org/10.1016/0010-2180(76)90062-6.

[26] M. Aniszewska, A. Gendek, Comparison of heat of combustion and calorific value of the cones and wood of selected forest trees species, For. Res. Pap. 75 (3) (2014) 231–236 [Online], https://depot.ceon.pl/handle/123456789/5332.

[27] ISO 12570:2000, Hygrothermal Performance of Building Materials and Products-Determination of Moisture Content by Drying at Elevated Temperature, ISO, Brussels, Belgium, 2000, 2000.

[28] M. Bonner, W. Węgrzyński, G. Rein, Visual fire power: an algorithm for measuring heat release rate of visible flames in camera footage, with applications in facade fire experiments, Fire Technol. 59 (2023) 191–215, https://doi.org/10.1007/s10694-022-01341-z.

[29] R.G. Gann, et al., Reconstruction of the fires and thermal environment in World Trade Center buildings 1, 2, and 7, Fire Technol. 49 (2013) 679–707.

[30] H.E. Nelson, Engineering View of the Fire of May 4, 1988 in the First Interstate Bank Building, 1989. Los Angeles, California (NIST IR 89-4061).

[31] B.R. Kirby, D.E. Wainman, L.N. Tomlinson, T.R. Kay, B.N. Peacock, Natural fires in large scale compartments, Int. J. Eng. Performance-Bases Fire Codes 1 (2) (1999) 43–58.

[32] D.C.O. Marney, L.J. Russell, R. Mann, Fire performance of wood (Pinus radiata) treated with fire retardants and a wood preservative, Fire Mater. 32 (6) (2008) 357–370, https://doi.org/10.1002/fam.973.

[33] F. Richter, F.X. Jervis, X. Huang, G. Rein, Effect of oxygen on the burning rate of wood, Combust. Flame 234 (2021), 111591, https://doi.org/10.1016/j.combustflame.2021.111591.

[34] H. Mitchell, R. Amin, M. Heidari, P. Kotsovinos, G. Rein, Structural hazards of smouldering fires in timber buildings, Fire Safe. J. 140 (2023) 103861, https://doi.org/10.1016/j.firesaf.2023.103861, 10/01/2023.

[35] J. Cuevas, J.L. Torero, C. Maluk, Flame extinction and burning behaviour of timber under varied oxygen concentrations, Fire Saf. J. 120 (2021), 103087, https://doi.org/10.1016/j.firesaf.2020.103087.

[36] A. Bartlett, A. Law, Influence of excess fuel from timber lined compartments, Construct. Build. Mater. 235 (2020), 117355, https://doi.org/10.1016/j.conbuildmat.2019.117355.

[37] J. Sjöström, D. Brandon, A. Temple, J. Anderson, R. McNamee, External fire plumes from mass timber compartment fires—comparison to test methods for regulatory

compliance of façades, Fire Mater. 47 (4) (2023) 433–444, https://doi.org/10.1002/fam.3129.

[38] A.I. Bartlett, R.M. Hadden, L.A. Bisby, A Review of factors affecting the burning behaviour of wood for application to tall timber construction, Fire Technol. 55 (1) (2019/01/01 2019) 1–49, https://doi.org/10.1007/s10694-018-0787-y.

[39] V. Gupta, J.L. Torero, J.P. Hidalgo, Burning dynamics and in-depth flame spread of wood cribs in large compartment fires, Combust. Flame 228 (2021) 42–56, https://doi.org/10.1016/j.combustflame.2021.01.031.